IEEE Access
Multidisciplinary | Rapid Review | Open Access Journal

Received November 10, 2019, accepted November 28, 2019, date of publication December 3, 2019,
date of current version December 17, 2019.

Digital Object Identifier 10.1109/ACCESS.2019.2957380

Method and Analysis of TOA-Based Localization in 5G Ultra-Dense Networks with Randomly Distributed Nodes

JIYAN HUANG[1], (Member, IEEE), JING LIANG[1], (Senior Member, IEEE), AND SHAN LUO[2]
[1]School of Information and Communication Engineering, University of Electronic Science and Technology of China, Chengdu 610054, China
[2]School of aeronautics and astronautics, University of Electronic Science and Technology of China, Chengdu 610054, China

Corresponding author: Jiyan Huang (huangjiyan@uestc.edu.cn)

This work was supported by the National Natural Science Foundation of China under Grant 61701079 and Grant 61731006.

ABSTRACT With the ever-growing number of networked devices and a higher likelihood of having line-of-sight communication most of the time, location estimation of a blind node in the 5th generation Ultra-Dense Networks (UDNs) system has gained considerable attention in recent years. One of main factors for accurate location estimates in 5G UDN is node randomness. Several location methods and their performance analyses have been addressed for localization in 5G UDN. Although the distribution of reference nodes (RNs) is considered in the literature, the information on spatial node distribution is only used to evaluate the average performance and is not utilized in the location methods. In this paper, a Cramer–Rao lower bound (CRLB) and three location estimators including the iterative, closed-form, and hybrid algorithms are proposed for localization in 5G UDN with randomly distributed RNs. Both range measurements and prior information on spatial node distribution are utilized for the proposed location methods and CRLB. Moreover, some characteristics of the CRLB for 5G UDN localization are derived in this paper. Detail comparison between the proposed CRLB and the previous performance study on CRLB for 5G UDN is given. Theoretical analysis proves that the proposed CRLB for the case with randomly distributed RNs is smaller than the average CRLB for the case with fixed location RNs. The top and bottom bounds of the proposed CRLB in the cases with low and high signal noise ratios are also given. Performance evaluation shows that the proposed methods perform better than the conventional methods only based on range measurements and can asymptotically attain the CRLB.

INDEX TERMS Wireless location, Cramer-Rao lower bound (CRLB), ultra-dense networks (UDNs), node distribution, time of arrival (TOA), convergence analysis.

I. INTRODUCTION

Wireless localization is of increasing importance for the 5th generation (5G) communications due to the expected rising demands of localization-based services in the future [1]. Location awareness, providing the physical location of every stationary or moving object or agent, will enhance the ability to deploy new services and better management of the overall 5G system. Beyond these, location-aware technologies can also enable a variety of other applications from precision agriculture, to intruder detection, health care, asset tracking, ocean data acquisition, or emergency services [2].

Location estimation of a blind node (BN) in wireless communication systems has gained considerable attention since the Federal Communication Commission (FCC) passed a mandate requiring cellular providers to generate accurate location estimates for Enhanced-911 services [3]. In the first phase of E-911 implementation, the wireless carrier must provide latitude and longitude estimates of the caller's position within an accuracy of 125 m root-mean-square error (RMSE) with 67 percent of the time in 2001 [3]. Subsequently, FCC launched the more stringent requirements in February 2015 on network operators asking for a 50-meter horizontal accuracy to be provided incrementally for 40%–80% of emergency calls especially for emergency response services [4]. Although Global Navigation Satellite Systems (GNSS) such as Global Positioning System (GPS) can meet the requirements of the positioning accuracy from FCC, its limitations, including high power consumption and suffering from degraded performance in

The associate editor coordinating the review of this manuscript and approving it for publication was Nitin Nitin.

outdoor rich-scattering scenarios and urban canyons, prevent GNSS from being applied in complex urban and indoor environments.

Much research and development work on localization techniques in wireless communication systems has been driven by E-911 mandate requirement. Several geolocation techniques including the time-of-arrival (TOA), the time-difference-of-arrival (TDOA), the angle-of-arrival (AOA), the signal strength (SS) based methods or hybrid location methods are used for wireless localization. Among these location techniques, a method based on TOA has attracted much attention [5]. In the multipath propagation environment, TOA is the measured propagation delay of the earliest distinguished path in the receivers. With the data of TOA, the location algorithms are used to estimate the position of the source in the location service center. Several TOA location algorithms have been addressed in the literature [5]–[7]. A cooperative localization strategy [5] based on TOA measurements is proposed for 5G Vehicular Ad hoc Network. The authors in [6] proposes a unified factor graph-based framework for passive localization in wireless sensor networks based on TOA measurements. Asymptotic Analysis for clock synchronization in TOA localization technique were presented in [7]. Due to the high positioning accuracy, the TOA localization technique has the greater chance to satisfy the FCC requirement. Therefore, this paper focuses on TOA based localization in 5G UDN system.

Many location methods assumed that the propagation is line-of-sight (LOS) have been firstly proposed in the literature [8]–[28]. The iterative methods [8]–[11] use the linearization techniques such as Taylor-series expansion, the steepest descent method, and Newton iteration to solve the nonlinear position problems. The closed-form methods have been developed for real-time implementation [12]–[15]. Caffery [12] uses the straight lines of position (LOP) rather than the circular LOP to determine the MS position. The divide and conquer method [13] utilizes the Fisher information to improve location accuracy. The spherical-interpolation (SI) method [14] transforms the nonlinear equations into a set of linear equations by introducing an extra variable. The SI method may lose the optimum as the relationship between the MS position and the extra variable is ignored. Chan and Ho [15] propose the two-step weighted least squares (WLS) method for TDOA localization technique based on maximum likelihood estimator (MLE) to improve the location accuracy of the SI method. Subsequently, a series of location methods [16]–[19] based on the two-step WLS estimator was proposed for various localization technique such as TOA, SS, and hybrid location methods. The location methods based on multidimensional scaling have been addressed in the literature [20]–[24]. Moreover, several performance analyses for wireless localization in LOS environments are presented in terms of Geometric Dilution of Precisions (GDOPs) and Cramer–Rao lower bounds (CRLBs) [15]–[18], [25]–[28].

One of main problems for accurate location estimates in early cellular wireless location systems is a Non-Line-of-Sight (NLOS) propagation, when the signal arrives at a reference node (RN) from reflections. There is no direct, or LOS, path. This often happens in an urban or indoor environment and may lead to severe degradations. Many positioning methods and characterizations for NLOS propagation have been addressed in the literature [29]–[41]. Broadly speaking, there are two ways to copy with NLOS errors. The first way is called geometric positioning methods [29]–[35]. These methods use geometric constraint conditions on NLOS propagation to suppress NLOS errors. The second way is Fingerprinting-based location methods depended on the learning theory and the information of training points [36]–[39]. The second way often works better than the geometric positioning methods at the cost of collecting training data. Some CRLBs of localization techniques for NLOS environments have been derived in the literature [35], [40]–[41].

Unfortunately, due to NLOS propagation and the limited number of RNs, it is difficult for localization techniques in early wireless communication systems such as 1G to 4G to fill the bill from FCC (50m with 40%-80% probability). Firstly, there is usually no LOS path in 1G to 4G communication systems. NLOS propagation may result in severe degradations. Take TOA localization technique as an example, NLOS propagation will add a large positive error in addition to standard measurement error from dozens of meters to thousands of meters. It is very difficult for geometric positioning methods [29]–[35] to obtain a good location estimate with such large NLOS error. Although Fingerprinting-based location methods [36]–[39] present good performance in the case of static environment, it is hardly applied in a practical system because of the high cost of building training database and the dynamic channel environment. The limited number of RNs in 1G to 4G wireless communication systems also degrades the location performance. To avoid the communication interference, the number of RNs communicating with a BN is usually small. Since lacking sufficient measurements collected from RNs, the positioning accuracy of 1G to 4G systems is not easy to meet the FCC requirement.

Ultra-Dense Networks (UDNs) infrastructure in 5G system overcomes the limitations of 1G to 4G communication systems and provides the potentiality to realize the higher location accuracy in meter level. The ever-growing number of networked devices in 5G and the emergence of ubiquitous networked objects as the Internet of Things mandate a new look into the conventional approaches proposed for localization in wireless communication networks [42]. With sufficient RNs and high carrier frequency such as 5G mm-wave, UDN in 5G has a higher likelihood of having LOS communication most of the time, both in indoor and outdoor scenarios [43]–[44]. Additionally, an increased number of RNs can help to improve the location performance.

Since UDN has natural advantage to provide the better location service, localization in UDN is becoming a new hot research area in recent years. Several location methods and their performance analyses have been addressed in the literature [42]–[45]. The authors in [45] utilize higher order Voronoi tessellations to provide ubiquitous localization services in UDN and derive the spatially averaged area of location region and localization error probability assuming that RNs are scattered according to a Poisson point process. A theoretical variance has been derived in [42] to provide a performance analysis for centroid localization in UDN. Both studies [42] and [45] are presented for range-free method. For range-based localization method in UDN, an AOA-based localization scheme combing edge cloud has been proposed in [44] and it has been verified by measurement results obtained from testbed. Subsequently, the authors in [43] derive a closed-form solution to the CRLB specific to 5G UDN. The spatial distribution of RNs was used in [43] to analyze the average performance of CRLB.

Despite these prior studies, two basic questions of localization in 5G UDN remain unanswered: what is the best achievable positioning accuracy of 5G UDN with randomly distributed RNs? and How to obtain the corresponding optimum positioning estimator using the prior information on RNs distribution? We believe that a systematic analysis of these problems is called for, and this paper reports our efforts along this direction. Main contributions of this paper are listed as follows:

(1) A CRLB and three location estimators including the iterative, closed-form, and hybrid methods are proposed in this paper for localization in 5G UDN with randomly distributed RNs. Our research results are totally different from current studies based on diverse assumptions. Current research including early studies on 1G to 4G systems [8]–[41] and recent studies on UDN [42]–[45] assumes that the RNs locate at fixed positions and the corresponding location algorithms [8]–[45] merely use range measurements or connectivity information to calculate the BN's position. Although node distributed model is considered in [42]–[43], [45], the information on spatial node distribution is only used to evaluate the average performance and is not utilized in the location methods. This paper assumes that the positions of RNs are subject to Gaussian model. In this paper, both range measurements and prior information on spatial node distribution are utilized for the proposed location methods and CRLB. Detailed comparison between the proposed CRLB and the average performance of traditional CRLB [43] will be presented in section III. To the best of our knowledge, this is first time in the literature to use statistical characteristics of RNs distribution to improve the positioning accuracy and derive the corresponding CRLB.

The determination of CRLB as an optimality criterion for the problem of mobile location is a very important issue because CRLB provides a benchmark to evaluate the performance of any unbiased location algorithm and determines the physical impossibility of the variance of an unbiased location algorithm being less than the bound. Many CRLBs have been addressed in the literature for various localization techniques and systems. CRLBs are firstly studied in the cellular location system (CLS) where both LOS [15]–[18] and NLOS [35], [40]–[41] cases are studied. Compared with CLS, the problem of sensor localization in a wireless sensor network (WSN) becomes more complex since the range measurements among all sensors are used rather than limited measurements between a BN and RNs for a CLS. The authors in [27] derived the CRLBs for the SS and TOA location technologies in WSNs. A more practical CRLB based on the distance-dependent variance model for range estimation noise was proposed in [46]. In [47], the clock biases were considered in the CRLB for distributed positioning in sensor network. The authors in [48] proposed the CRLB for RN-free localization and derived the lower and upper bounds on the CRLB. CRLBs considering the uncertainties in the positions of RNs were presented in [49]–[50]. Furthermore, the authors in [51] derived the CRLBs for WSN considering both the NLOS propagation and RN location error. Beside those studies, some CRLBs [41], [52] were proposed to evaluate the performance of the location methods based on prior user location knowledge.

The main difference of the proposed CRLB and previous CRLBs is that the distribution of RNs has not been considered in previous CRLBs [15]–[18], [27], [35], [40]–[41], [46]–[52] whereas both range measurements and statistical characteristics of RNs distribution are used in the proposed CRLB. With the ever-growing number of networked devices in UDN, Node randomness becomes more and more important in wireless localization of UDN. The main contribution of the paper is that we use statistical characteristics of RNs distribution to improve the positioning accuracy and derive the corresponding CRLB which have not been addressed in previous studies. An analysis that incorporates the distribution of RNs, prior user location knowledge, and RN location error will be left for a future study.

(2) Some characteristics of the CRLB for 5G UDN localization are derived in this paper. Proposition 1 proves that the proposed CRLB for the case with randomly distributed RNs is smaller than the average CRLB [43] for the case with fixed location RNs. The conclusion shows that the location system with the prior information on the node distribution has the higher positioning accuracy than the traditional location technique assuming that RNs locates at fixed positions. This implies that statistical characteristics of RNs distribution can help to improve the system performance. Proposition 2 presents the top and bottom bounds of the proposed CRLB in the cases with low and high signal noise ratios (SNRs).

(3) Based on MLE, three location algorithms including the iterative, closed-form, and hybrid methods using both the range measurements and RN distribution are proposed in this paper to reduce the location error. Firstly, theoretical analysis in Proposition 3 shows that the cost functions of both the proposed and traditional iterative methods are a convex

function for the case of good GDOP and enough large RNs whereas it is a non-convex function for the case of bad GDOP and small numbers of RNs. This means that the iterative methods can get good performance with sufficiently large RNs whereas bad GDOP or small number of RNs may lead to the divergence of the iterative method. Thus, a hybrid method combing the proposed iterative method and closed-form solution is given. In the proposed hybrid method, the iterative method is used to provide the estimate results with high positioning precision while its convergence is guaranteed by the closed-form solution. The GDOP test and convergence test are proposed in the hybrid method to provide a compromise between the positioning accuracy and convergence of the method. Performance evaluation shows that the proposed methods perform better than the traditional methods only based on range measurements and can asymptotically attain the CRLB.

This paper is organized as follows. Signal model and some basic notations are presented in section II. In section III, the paper derives a CRLB for 5G UDN with randomly distributed RNs. Some characteristics of the CRLBs are also discussed in this section. Section IV proposes three location methods based on MLE using both range measurements and RN distribution. Section V records the performance evaluation of the proposed CRLB and location methods. Conclusions of this paper are given in Section VI.

II. SYSTEM MODEL

The basic system models are briefly introduced in this section. TOA measurement model is first presented and then the model of RNs' distribution is summarized at the end of this section.

Assuming that (x, y) is the position of a BN and (x_i, y_i) is the position of the ith RN in a N-RNs system. The BN position is an unknown parameter to be estimated. This paper considers both range measurements and node randomness. The paper focuses on the TOA based localization technique where the TOA measurements are used to locate a BN. The TOA measurement $\widehat{t}_i$ is the transmission time between BN and RN i. Denote the measurement with noise of $\{*\}$ as $\left\{\widehat{*}\right\}$. The range measurement $\widehat{r}_i$ from the corresponding TOA measurement $\widehat{t}_i$ is modeled as:

$$\widehat{r}_i = c\widehat{t}_i = r_i + n_i = \sqrt{(x - x_i)^2 + (y - y_i)^2} + n_i \quad (1)$$

where c is the speed of light, r_i is the true distance between the BN and RN i. Assuming that the signal propagations between the BN and all RNs are LOS such that n_i is a zero-mean Gaussian random process with variance σ^2. This assumption is reasonable and widely used in the 5G UDN [43]–[44]. Since 5G UDN usually operates at a mm-wave carrier frequency in the range of 30-300Ghz with large bandwidth, both LOS and NLOS paths coexist in the received signals. It is easy to extract LOS signal from TOA measurements since the first path of TOA measurements is LOS signal.

Node randomness is another principal element for the performance of localization method. Various node distributions are proposed in the literature based on different assumptions. Uniform distribution is first addressed in the literature to build node distributed model where sensor nodes are assumed to be uniformly distributed in a disk of radius R [42]–[43], [45]. However, over the past years it has been recognized that the assumption of uniformly distributed nodes is rather implausible for real, deployed wireless networks [53]–[54]. And in fact, node spatial distribution relies on many factors, such as deployment method, the surroundings of nodes, nodes motion, communication protocol, and even the power status of nodes. According to the central limit theorem, the actual node location will follow Gaussian distribution [53]–[54]. In this model, N RNs place around a BN according to a two-dimensional Gaussian spatial distribution with mean $[x, y]$ and a covariance matrix $\sigma_p^2\mathbf{I}$. The probability that a RN locates at (x_i, y_i) can be described by probability density function (PDF) [54]:

$$f(x_i, y_i) = \frac{1}{2\pi\sigma_p^2} \exp\left(-\frac{(x_i - x)^2 + (y_i - y)^2}{2\sigma_p^2}\right) \quad (2)$$

where σ_p is the standard deviation (std) of node distribution which determine the distributed range of RNs. It should be noted that (2) is based on cartesian coordinates. For polar coordinates, the PDF (2) can be written as:

$$f(r_i) = \frac{1}{\sigma_p^2} \exp\left(-\frac{r_i^2}{2\sigma_p^2}\right) r_i \quad r_i > 0$$
$$f(\phi_i) = \frac{1}{2\pi} \quad -\pi \le \phi_i < \pi \quad (3)$$

where r_i is the range between the ith RN and BN which has been defined in (1). $\phi_i = a\cos\left((x - x_i)/r_i\right)$ is the azimuth angle of RN i with respect to BN. Fig. 1 shows an example of Gaussian node distribution with the number of RNs is 60. Both Fig. 1 and equation (3) show that RNs will appear around BN with equal probability in different directions and $f(x_i, y_i)$ depends only on the distance between RD and BD. This also implies that a RN near the BN may have the higher probability than a farther RN.

III. THEORETICAL ANALYSIS OF TOA BASED LOCALIZATION TECHNIQUE FOR UDN WITH RANDOMLY DISTRIBUTED NODES

This section investigates the performance of TOA based localization technique for UDN with randomly distributed nodes in terms of CRLB. The CRLB is very important for parameter estimation since it provides a benchmark to evaluate the performance of any unbiased estimator.

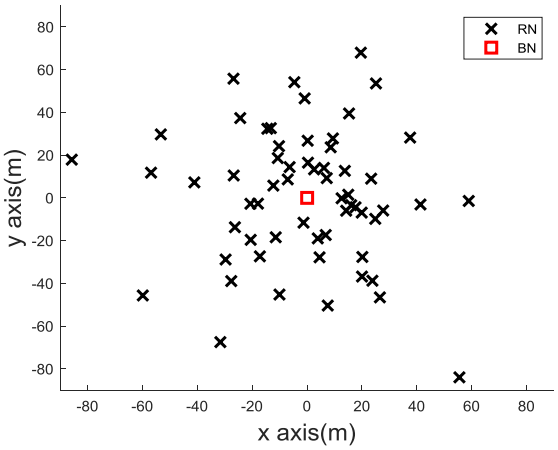

FIGURE 1. An example of Gaussian node distribution.

Let $\mathbf{r} = \left[\widehat{r}_1 \cdots \widehat{r}_N\right]^T$ be a range measurement vector and $\boldsymbol{\theta} = \left[x\ y\right]^T$ is an unknown parameter vector to be estimated. It is assumed that the PDF $f(\mathbf{r};\boldsymbol{\theta})$ satisfies the "regularity" conditions [55]:

$$E\left[\frac{\partial \ln f(\mathbf{r};\boldsymbol{\theta})}{\partial \boldsymbol{\theta}}\right] = 0 \text{ for all } \boldsymbol{\theta} \tag{4}$$

where the expectation is taken with respect to $f(\mathbf{r};\boldsymbol{\theta})$. Then, The CRLB matrix is defined as the inverse of the Fisher information matrix (FIM) $\mathbf{J}_{\boldsymbol{\theta}}$:

$$E\left(\left(\widehat{\theta} - \boldsymbol{\theta}\right)\left(\widehat{\theta} - \boldsymbol{\theta}\right)^T\right) \geq \mathbf{J}_{\boldsymbol{\theta}}^{-1} \tag{5}$$

where $\widehat{\theta}$ is an estimate of $\boldsymbol{\theta}$.

The FIM is determined by [55]:

$$\mathbf{J}_{\boldsymbol{\theta}} = E\left[\frac{\partial \ln f(\mathbf{r};\boldsymbol{\theta})}{\partial \boldsymbol{\theta}}\left(\frac{\partial \ln f(\mathbf{r};\boldsymbol{\theta})}{\partial \boldsymbol{\theta}}\right)^T\right] \tag{6}$$

A. THE AVERAGE CRLB FOR THE CASE WITH FIXED LOCATION RNS [43]

The CRLBs of TOA localization technique have been widely studied in [18], [43] for the case with fixed RNs. In this assumption, the positions of RNs are deterministic parameters and its PDF can be written as:

$$f(\mathbf{r};\boldsymbol{\theta}) = \prod_{i=1}^{N} f\left(\widehat{r}_i\right) \tag{7}$$

where $f\left(\widehat{r}_i\right)$ is the PDF of range measurement $\widehat{r}_i$ and can be obtained from TOA model in (1):

$$f\left(\widehat{r}_i\right) = \frac{1}{\sqrt{2\pi}\sigma}\exp\left(-\frac{\left(\widehat{r}_i - r_i\right)^2}{2\sigma^2}\right) \tag{8}$$

The above equation shows that the PDF for the case with fixed location RNs totally depends on the range measurements and has nothing to do with the distribution of RNs.

Substituting (7) and (8) into (6), gives:

$$\mathbf{J}_{\boldsymbol{\theta}} = \mathbf{H}\mathbf{Q}^{-1}\mathbf{H}^T \tag{9}$$

where $\mathbf{Q} = \sigma^2\mathbf{I}$, $\mathbf{I}$ is an identity matrix, $\frac{\partial r_i}{\partial x} = \cos\phi_i = \frac{x - x_i}{r_i}$, $\frac{\partial r_i}{\partial y} = \sin\phi_i = \frac{y - y_i}{r_i}$, and

$$\mathbf{H} = \begin{bmatrix} \frac{\partial r_1}{\partial x} & \cdots & \frac{\partial r_N}{\partial x} \\ \frac{\partial r_1}{\partial y} & \cdots & \frac{\partial r_N}{\partial y} \end{bmatrix} \tag{10}$$

It should be noted that the derivation of (9) assumes that the positions of RNs are deterministic parameters and the expectation in (6) only acts on range measurements $\widehat{r}_i$.

Equation (10) can be further simplified as

$$\mathbf{J}_{\boldsymbol{\theta}} = \frac{1}{\sigma^2}\begin{bmatrix} \sum_{i=1}^{N}\cos^2\phi_i & \sum_{i=1}^{N}\cos\phi_i\sin\phi_i \\ \sum_{i=1}^{N}\cos\phi_i\sin\phi_i & \sum_{i=1}^{N}\sin^2\phi_i \end{bmatrix} \tag{11}$$

From the second moment matrix inversion formula [56],

$$\begin{bmatrix} a & b \\ c & d \end{bmatrix}^{-1} = \frac{1}{ad - bc}\begin{bmatrix} d & -b \\ -c & a \end{bmatrix} \tag{12}$$

$\mathbf{J}_{\boldsymbol{\theta}}^{-1}$ can be expressed as:

$$\mathbf{J}_{\boldsymbol{\theta}}^{-1} = \frac{\sigma^2}{\sum_{i=1}^{N}\cos^2\phi_i\sum_{i=1}^{N}\sin^2\phi_i - \left(\sum_{i=1}^{N}\cos\phi_i\sin\phi_i\right)^2} \times \begin{bmatrix} \sum_{i=1}^{N}\sin^2\phi_i & -\sum_{i=1}^{N}\cos\phi_i\sin\phi_i \\ -\sum_{i=1}^{N}\cos\phi_i\sin\phi_i & \sum_{i=1}^{N}\cos^2\phi_i \end{bmatrix} \tag{13}$$

The CRLB is

$$Tr\left\{\mathbf{J}_{\boldsymbol{\theta}}^{-1}\right\} = \frac{N\sigma^2}{\sum_{i=1}^{N}\cos^2\phi_i\sum_{i=1}^{N}\sin^2\phi_i - \left(\sum_{i=1}^{N}\cos\phi_i\sin\phi_i\right)^2} = \frac{N\sigma^2}{\sum_{i=1}^{N}\sum_{\substack{j=1 \\ i\neq j}}^{N}\left(\cos^2\phi_i\sin^2\phi_i - \cos\phi_i\sin\phi_i\cos\phi_j\sin\phi_j\right)} \tag{14}$$

It can be seen from (14) that the CRLB for the case with fixed location RNs depends on the variance σ^2 of range

measurement noise and GDOP ($\cos\phi_i$ and $\sin\phi_i$). Different GDOPs will lead to various CRLBs.

To evaluate the average performance, the average CRLB is defined as [43]:

$$CR_f = E\left[tr\left\{\mathbf{J}_{\boldsymbol{\theta}}^{-1}\right\}\right] = E\left[\frac{N\sigma^2}{\sum_{i=1}^{N}\sum_{\substack{j=1\\ i\neq j}}^{N}\left(\cos^2\phi_i\sin^2\phi_i - \cos\phi_i\sin\phi_i\cos\phi_j\sin\phi_j\right)}\right] \tag{15}$$

Obviously, (15) has not closed-form solution and further approximation should be developed for performance analysis. With a sufficiently large N, the expected mean can be replaced with the sample mean and the average CRLB is approximated as [43]:

$$CR_f \approx \frac{N\sigma^2}{E\left[\sum_{i=1}^{N}\sum_{\substack{j=1\\ i\neq j}}^{N}\left(\cos^2\phi_i\sin^2\phi_i - \cos\phi_i\sin\phi_i\cos\phi_j\sin\phi_j\right)\right]} = \frac{4\sigma^2}{N-1} \tag{16}$$

It can be seen from the above derivation that the PDF of RNs' distribution (3) is not applied to calculate the CRLB (14) whereas it is utilized to compute the average performance (16) of CRLB.

B. THE PROPOSED CRLB FOR THE CASE WITH RANDOMLY DISTRIBUTED RNS

The CRLB for the case with randomly distributed RNs is derived in this subsection. From (2) and (8), the joint conditional PDF $f(\mathbf{r};\boldsymbol{\theta})$ can be written as:

$$f(\mathbf{r};\boldsymbol{\theta}) = \prod_{i=1}^{N} f\left(\widehat{r}_i, x_i, y_i; \boldsymbol{\theta}\right) \tag{17}$$

where

$$f\left(\widehat{r}_i, x_i, y_i; \boldsymbol{\theta}\right) = f\left(\widehat{r}_i\right) f(x_i, y_i) \tag{18}$$

$f(x_i, y_i)$ describes the node distributed probability which is defined in (2) and $f\left(\widehat{r}_i\right)$ is the PDF of $\widehat{r}_i$.

Compared (7) with (18), the proposed CRLB assumes that the position of RNs (x_i, y_i) is a random parameter and the expectation in (6) will act on both $\widehat{r}_i$ and (x_i, y_i) in the proposed CRLB.

The log of $f(\mathbf{r};\boldsymbol{\theta})$ is

$$\begin{aligned}\ln f(\mathbf{r};\boldsymbol{\theta}) &= \sum_{i=1}^{N}\ln f\left(\widehat{r}_i, x_i, y_i; \boldsymbol{\theta}\right)\\ &= \sum_{i=1}^{N}\left(\ln f\left(\widehat{r}_i\right) + \ln f(x_i, y_i)\right)\end{aligned} \tag{19}$$

Substituting (19) into $\partial \ln f(\mathbf{r};\boldsymbol{\theta})/\partial\theta_i$, gives:

$$\begin{aligned}\frac{\partial \ln f(\mathbf{r};\boldsymbol{\theta})}{\partial x} &= \sum_{i=1}^{N}\left(\frac{n_i}{\sigma^2}\cos\phi_i - \frac{x - x_i}{\sigma_p^2}\right)\\ \frac{\partial \ln f(\mathbf{r};\boldsymbol{\theta})}{\partial y} &= \sum_{i=1}^{N}\left(\frac{n_i}{\sigma^2}\sin\phi_i - \frac{y - y_i}{\sigma_p^2}\right)\end{aligned} \tag{20}$$

Since the coefficients $1/\left(2\pi\sigma_p^2\right)$ and $1/\left(\sqrt{2\pi}\sigma\right)$ in the PDFs $f(x_i, y_i)$ and $f\left(\widehat{r}_i\right)$ are constants, differentiating them with respect to x and y will lead to zero. Thus, $1/\left(2\pi\sigma_p^2\right)$ and $1/\left(\sqrt{2\pi}\sigma\right)$ is ignored in the derivation of (20).

The expectations of the above equations are:

$$\begin{aligned}E\left[\frac{\partial \ln f(\mathbf{r};\boldsymbol{\theta})}{\partial x}\right] &= \sum_{i=1}^{N}\left(\frac{E[n_i]}{\sigma^2}E[\cos\phi_i] - \frac{E[x - x_i]}{\sigma_p^2}\right) = 0\\ E\left[\frac{\partial \ln f(\mathbf{r};\boldsymbol{\theta})}{\partial y}\right] &= \sum_{i=1}^{N}\left(\frac{E[n_i]}{\sigma^2}E[\sin\phi_i] - \frac{E[y - y_i]}{\sigma_p^2}\right) = 0\end{aligned} \tag{21}$$

It can be observed from (21) that the case of Gaussian node distribution satisfies the "regularity" conditions which means there exists a CRLB for Gaussian distributed nodes.

Substituting (20) into $E\left[\left(\partial \ln f(\mathbf{r};\boldsymbol{\theta})/\partial x\right)^2\right]$, gives:

$$\begin{aligned}E\left[\left(\frac{\partial \ln f(\mathbf{r};\boldsymbol{\theta})}{\partial x}\right)^2\right] &= E\left[\sum_{i=1}^{N}\left(\frac{n_i\cos\phi_i}{\sigma^2} - \frac{x - x_i}{\sigma_p^2}\right)^2\right]\\ &+ E\left[\sum_{i=1}^{N}\sum_{\substack{j=1\\ i\neq j}}^{N}\left(\frac{n_i\cos\phi_i}{\sigma^2} - \frac{x - x_i}{\sigma_p^2}\right)\left(\frac{n_j\cos\phi_j}{\sigma^2} - \frac{x - x_j}{\sigma_p^2}\right)\right]\\ &= \sum_{i=1}^{N}\left(\frac{E\left[n_i^2\right]E\left[\cos^2\phi_i\right]}{\sigma^4} - 2\frac{E[n_i]E[\cos\phi_i(x - x_i)]}{\sigma^2\sigma_p^2}\right.\\ &\left. + \frac{E\left[(x - x_i)^2\right]}{\sigma_p^4}\right)\end{aligned} \tag{22}$$

Noting that

$$\begin{aligned}E\left[\cos^2\phi_i\right] &= \int_{-\pi}^{+\pi}\cos^2\phi_i f(\phi_i)d\phi_i = \int_{-\pi}^{+\pi}\frac{\cos^2\phi_i}{2\pi}d\phi_i\\ &= \frac{1}{2\pi}\left(\frac{1}{4}\sin(2\phi_i) + \frac{\phi_i}{2}\right)\Big|_{-\pi}^{+\pi} = \frac{1}{2}\end{aligned} \tag{23}$$

It can be obtained from (2), (8), (22), and (23) that

$$E\left[\left(\frac{\partial \ln f(\mathbf{r};\boldsymbol{\theta})}{\partial x}\right)^2\right] = \sum_{i=1}^{N}\left(\frac{\sigma^2}{2\sigma^4}+\frac{\sigma_p^2}{\sigma_p^4}\right) = N\left(\frac{1}{2\sigma^2}+\frac{1}{\sigma_p^2}\right) \tag{24}$$

Similarly, we have:

$$E\left[\left(\frac{\partial \ln f(\mathbf{r};\boldsymbol{\theta})}{\partial y}\right)^2\right] = N\left(\frac{1}{2\sigma^2}+\frac{1}{\sigma_p^2}\right) \tag{25}$$

$$E\left[\frac{\partial \ln f(\mathbf{r};\boldsymbol{\theta})}{\partial x}\frac{\partial \ln f(\mathbf{r};\boldsymbol{\theta})}{\partial y}\right] = 0 \tag{26}$$

Finally, the proposed CRLB is derived as:

$$CR_r = Tr\left\{\mathbf{J}_{\boldsymbol{\theta}}^{-1}\right\} = \frac{2}{N\left(\frac{1}{2\sigma^2}+\frac{1}{\sigma_p^2}\right)} = \frac{4\sigma^2\sigma_p^2}{N\left(\sigma_p^2+2\sigma^2\right)} \tag{27}$$

Remark 1: It should be noted that CR_f and CR_r are totally different CRLBs based on diverse assumptions. The former assumes that the RNs locate at fixed positions and the corresponding location algorithms [8]–[45] merely use range measurements or connectivity information to calculate the BN's position. The information on spatial node distribution is only used to evaluate the average performance [42]–[43], [45] and is not used in the location methods [8]–[45] . The latter assumes that the positions of RNs are subject to Gaussian model. Both range measurements and prior information on spatial node distribution are utilized for the proposed location methods and CRLB.

C. CHARACTERISTICS OF THE PROPOSED CRLB

The characteristics of the proposed CRLB are provided in the following Propositions.

Proposition 1

The CRLB for the case with randomly distributed RNs is smaller than the average CRLB for the case with fixed location RNs.

$$CR_r = \frac{4\sigma^2\sigma_p^2}{N\left(\sigma_p^2+2\sigma^2\right)} < CR_f = \frac{4\sigma^2}{N-1} \tag{28}$$

Proof: Comparing (16) with (27), gives:

$$\frac{CR_r}{CR_f} = \frac{4\sigma^2\sigma_p^2}{N\left(\sigma_p^2+2\sigma^2\right)} \Big/ \frac{4\sigma^2}{N-1} = \frac{N-1}{N\left(1+2\sigma^2/\sigma_p^2\right)} \tag{29}$$

Obviously,

$$N\left(1+2\sigma^2/\sigma_p^2\right) - (N-1) = N2\sigma^2/\sigma_p^2 + 1 > 0 \tag{30}$$

Substituting (30) into (29), gives:

$$\frac{CR_r}{CR_f} = \frac{N-1}{N\left(1+2\sigma^2/\sigma_p^2\right)} < 1 \tag{31}$$

Equation (28) holds.

Proposition 1 shows that the location system with the prior information on the node distribution has the higher positioning accuracy than the traditional location technique assuming that RNs locates at fixed positions. This implies that statistical characteristics of RNs distribution can help to improve the system performance. In next section, three novel location methods based MLE are proposed to improve the accuracy of BN location using statistical characteristics of RNs distribution.

Proposition 2

In the case of high SNR, the proposed CRLB can be approximated as:

$$CR_{r\_h} \approx \frac{4\sigma^2}{N} \tag{32}$$

In the case of low SNR, the proposed CRLB can be approximated as:

$$CR_{r\_low} \approx \frac{4\bar{r}^2}{N(1+\pi)} \tag{33}$$

where $\bar{r}$ is the mean range of RNs between BN.

Proof: Since $\bar{r}$ is the mean range of r_i,

$$\bar{r} \approx E[r_i] \approx \int_0^{+\infty} r_i f(r_i)\, dr_i \tag{34}$$

It can be seen from (3) that r_i is subject to Rayleigh distribution. Based on the properties of Rayleigh PDF [55], we have:

$$\bar{r} \approx E[r_i] = \sqrt{\frac{\pi\sigma_p^2}{2}} \tag{35}$$

Substituting (35) into (27), gives

$$CR_r \approx \frac{4\sigma^2}{N\left(1+\pi r_e^2\right)} \tag{36}$$

where $r_e = \sigma/\bar{r}$ is ratio of range measurement error σ to the mean range $\bar{r}$. Obviously, the range measurement error will not exceed the transmission range and $0 < \sigma < \bar{r}$.

With high SNR, $\sigma \to 0$ and $r_e \approx 0$. Thus, (36) becomes:

$$CR_r \approx \frac{4\sigma^2}{N} \tag{37}$$

With low SNR, $\sigma \to \bar{r}$ and $r_e \approx 1$. Thus, (36) becomes:

$$CR_r \approx \frac{4\bar{r}^2}{N(1+\pi)} \tag{38}$$

Fig. 2 shows the three CRLBs versus different range error ratios r_e when the number of RNs is 20 and $\sigma_p = 30m$. It can be seen from figure that CR_r matches well with CR_{r_h} in the case of high SNR ($r_e \leq 0.15$). For the case with low SNR,

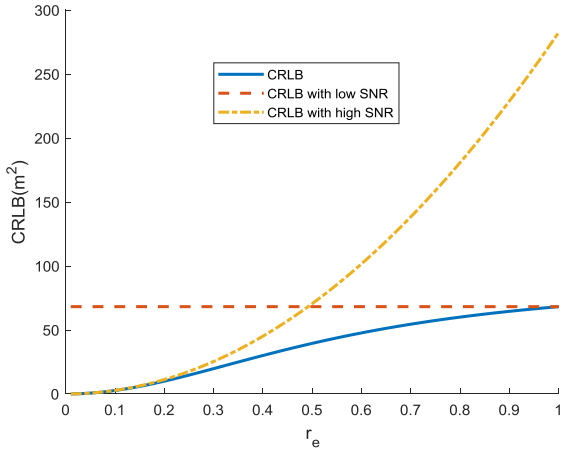

FIGURE 2. CRLB versus different r_e.

CR_r asymptotically reaches CR_{r_low} as $\sigma \to \bar{r}$. Fig. 2 proves the effectiveness of Proposition 2.

The proposed CRLB (27) shows that the positioning accuracy of UDNs depends on the number of RNs, range measurement noise and spatial node distribution. Proposition 2 further implies that the CRLB mainly lies on range measurements rather than the prior information of node distribution in high SNR situation. In the case of low SNR, the range estimate becomes worse and makes substantially less contribution to the performance. In the extreme situation, the CRLB (33) totally depends $\bar{r}$ and N. In this case, range-based location technique degrades into range-free method.

IV. MLE OF TOA BASED LOCALIZATION IN UDN WITH RANDOMLY DISTRIBUTED RNS

The proposed CRLB in section III indicates the best achievable positioning accuracy of TOA based localization technique in UDN with randomly distributed RNs. This section proposes three novel location methods based on MLE which answer another unsolved problem: how to attain the CRLB using both TOA measurements and statistical information on node distribution?

It is well known that the MLE is asymptotically unbiased and can asymptotically attain the CRLB with sufficiently large measurements. It is asymptotically efficient and optimal [55].

The MLE is found by maximizing the PDF (17) or, equivalently, by maximizing the likelihood function.

$$\begin{aligned} J_r(\boldsymbol{\theta}) &= J_f(\boldsymbol{\theta}) + J_s(\boldsymbol{\theta}) = \sum_{i=1}^{N} \ln f\left(\widehat{r}_i\right) + \sum_{i=1}^{N} \ln f\left(x_i, y_i\right) \\ &= -\left(N \ln\left(\sqrt{2\pi}\sigma\right) + \sum_{i=1}^{N} \frac{\left(\widehat{r}_i - r_i\right)^2}{2\sigma^2}\right) \\ &\quad -\left(N \ln\left(2\pi\sigma_p^2\right) + \sum_{i=1}^{N} \frac{r_i^2}{2\sigma_p^2}\right) \end{aligned} \tag{39}$$

Noting that the first term $J_f(\boldsymbol{\theta})$ is the likelihood function for the case with fixed location RNs.

This section proposes three novel location algorithms for the case with randomly distributed RNs and makes a convergence analysis for the cost function (39) of the proposed iterative method. The proposed methods are based on MLE and use statistical characteristics of RNs distribution as prior information to improve the accuracy of BN location. Based on MLE, an iterative method of Newton-Raphson is proposed for the case with good GDOP and a closed-form solution using two steps WLS is developed to guarantee the convergence of Newton-Raphson method in bad channel situation.

A. ITERATIVE METHOD OF NEWTON-RAPHSON FOR THE CASE WITH RANDOMLY DISTRIBUTED RNS

A novel iterative method based on MLE and the distribution of RNs is proposed in this subsection.

The MLE attempts to maximize the likelihood function (39) by finding a zero of the derivative function. From (39), we have:

$$\begin{aligned} \frac{\partial J_r(\boldsymbol{\theta})}{\partial x} &= \sum_{i=1}^{N} \left(\frac{\widehat{r}_i - r_i}{\sigma^2 r_i} - \frac{1}{\sigma_p^2}\right)(x - x_i) = 0 \\ \frac{\partial J_r(\boldsymbol{\theta})}{\partial y} &= \sum_{i=1}^{N} \left(\frac{\widehat{r}_i - r_i}{\sigma^2 r_i} - \frac{1}{\sigma_p^2}\right)(y - y_i) = 0 \end{aligned} \tag{40}$$

Equivalently, the following equations hold:

$$\begin{aligned} g_1(\boldsymbol{\theta}) &= \frac{\widehat{r}_1 - r_1}{\sigma^2} - \frac{r_1}{\sigma_p^2} = 0 \\ &\vdots \\ g_N(\boldsymbol{\theta}) &= \frac{\widehat{r}_N - r_N}{\sigma^2} - \frac{r_N}{\sigma_p^2} = 0 \end{aligned} \tag{41}$$

Assuming that there is an initial guess for the solution to (41). Using the first order approximation of Taylor expansion:

$$\begin{aligned} g_i(\boldsymbol{\theta}) \approx g_i(\boldsymbol{\theta}_0) &+ \frac{\partial g_i(\boldsymbol{\theta})}{\partial x}\Big|_{\boldsymbol{\theta}=\boldsymbol{\theta}_0}(x - x_0) \\ &+ \frac{\partial g_i(\boldsymbol{\theta})}{\partial y}\Big|_{\boldsymbol{\theta}=\boldsymbol{\theta}_0}(y - y_0) \approx 0 \end{aligned} \tag{42}$$

where

$$\begin{aligned} \frac{\partial g_i(\boldsymbol{\theta})}{\partial x} &= -\left(\frac{1}{\sigma^2} + \frac{1}{\sigma_p^2}\right)\frac{x - x_i}{r_i} \\ \frac{\partial g_i(\boldsymbol{\theta})}{\partial y} &= -\left(\frac{1}{\sigma^2} + \frac{1}{\sigma_p^2}\right)\frac{y - y_i}{r_i} \end{aligned} \tag{43}$$

Expressing (42) in matrix form, gives:

$$\mathbf{P}\left(\boldsymbol{\theta}_{k+1} - \boldsymbol{\theta}_k\right) = -\mathbf{D} \tag{44}$$

where $\boldsymbol{\theta}_k$ is the kth iterative estimate of $\boldsymbol{\theta}$.

$$\mathbf{P} = \begin{bmatrix} \frac{\partial g_1(\boldsymbol{\theta})}{\partial x} & \frac{\partial g_1(\boldsymbol{\theta})}{\partial y} \\ \vdots & \vdots \\ \frac{\partial g_N(\boldsymbol{\theta})}{\partial x} & \frac{\partial g_N(\boldsymbol{\theta})}{\partial y} \end{bmatrix} \Big|_{\boldsymbol{\theta}=\boldsymbol{\theta}_k},$$
$$\mathbf{D} = \begin{bmatrix} g_1(\boldsymbol{\theta}_k) & g_2(\boldsymbol{\theta}_k) \end{bmatrix}^T$$

Since $\mathbf{P}$ is the derivate of the log-likelihood function, we find the MLE as:

$$\boldsymbol{\theta}_{k+1} = \boldsymbol{\theta}_k - \left(\mathbf{P}^T\mathbf{P}\right)^{-1}\mathbf{P}^T\mathbf{D} \tag{45}$$

Note that at convergence $\boldsymbol{\theta}_{k+1} = \boldsymbol{\theta}_k$, and from (41) $g_1(\boldsymbol{\theta}_k) = g_2(\boldsymbol{\theta}_k) = 0$, as desired.

Other convex optimization tools such as MATLAB package CVX [57] also can be used to solve the cost function (39). It will be proved in the next subsection that the cost function (39) is a convex function only for the case of good GDOP and enough large N. This means that both the proposed iterative method and other convex optimization tools may diverge in bad channel situation. A hybrid method is proposed in section.IV(C) to void divergency.

B. CONVERGENCE ANALYSIS OF THE PROPOSED ITERATIVE METHOD

Convergence analysis is a very important issue for the iterative method since the iterations may not converge. This subsection provides a convergence analysis for the proposed iterative method. In fact, the convergence analysis is equivalent to solve the following problem: the cost function (39) of the proposed iterative method is a convex or non-convex function. The following Proposition tries to find the answer.

Proposition 3

The cost function (39) of the proposed iterative method is a convex function for the case of good GDOP and enough large N whereas it is a non-convex function for the case of bad GDOP and small N.

Proof: Differentiating (39) with respect to x produces

$$\frac{\partial J_r(\boldsymbol{\theta})}{\partial x} = \frac{\partial J_f(\boldsymbol{\theta})}{\partial x} + \frac{\partial J_s(\boldsymbol{\theta})}{\partial x} \tag{46}$$

where

$$\frac{\partial J_f(\boldsymbol{\theta})}{\partial x} = \sum_{i=1}^{N} \frac{\widehat{r}_i - r_i}{\sigma^2}\frac{x - x_i}{r_i}, \frac{\partial J_s(\boldsymbol{\theta})}{\partial x} = -\sum_{i=1}^{N}\frac{x - x_i}{\sigma_p^2} \tag{47}$$

The second derivative of $J_s(\boldsymbol{\theta})$ with respect to x can be written as:

$$\frac{\partial^2 J_s(\boldsymbol{\theta})}{\partial x^2} = -\frac{N}{\sigma_p^2} < 0 \tag{48}$$

Obviously, $J_s(\boldsymbol{\theta})$ is a convex function. Thus, the convergence analysis becomes a problem determining whether $J_f(\boldsymbol{\theta})$ is a convex function.

The second derivative of $J_f(\boldsymbol{\theta})$ with respect to x can be written as:

$$\begin{aligned}\frac{\partial^2 J_f(\boldsymbol{\theta})}{\partial x^2} &= \frac{1}{\sigma^2}\sum_{i=1}^{N}\left(\frac{\left(-\frac{\partial r_i}{\partial x}(x - x_i) + \left(\widehat{r}_i - r_i\right)\right) r_i}{r_i^2}\right. \\ &\quad \left.\times \frac{-\left(\widehat{r}_i - r_i\right)(x - x_i)\frac{\partial r_i}{\partial x}}{r_i^2}\right) \\ &= \frac{1}{\sigma^2}\sum_{i=1}^{N}\left(-\cos^2\phi_i + n_i\left(\frac{\sin\phi_i}{r_i}\right)^2\right)\end{aligned} \tag{49}$$

The above equation shows that $\partial^2 J_f(\boldsymbol{\theta})/\partial x^2$ depends on the range measurement noise n_i, the number of RNs N, and GDOP ($\sin\phi_i$ and $\cos\phi_i$). Since n_i is a Gaussian variable with zero mean and $-\infty < n_i < +\infty$, the value of $\partial^2 J_f(\boldsymbol{\theta})/\partial x^2$ is uncertainty.

For the case of good GDOP and enough large N,

$$\begin{aligned}\frac{\partial^2 J_f(\boldsymbol{\theta})}{\partial x^2} &= \frac{1}{\sigma^2}\left(-\sum_{i=1}^{N}\cos^2\phi_i + \sum_{i=1}^{N} n_i\left(\frac{\sin\phi_i}{r_i}\right)^2\right) \\ &\approx -\frac{1}{\sigma^2}\sum_{i=1}^{N}\cos^2\phi_i < 0\end{aligned} \tag{50}$$

Thus, the cost function (39) of the proposed iterative method is a convex function for the case of good GDOP and enough large N. Otherwise, $\partial^2 J_f(\boldsymbol{\theta})/\partial x^2$ may be greater than 0 which may lead to a non-convex cost function of the iterative method. Using the similar derivation, $\partial^2 J_f(\boldsymbol{\theta})/\partial y^2$ has the same conclusion. Proposition 3 holds.

Remark 2: It should be noted that $J_f(\boldsymbol{\theta})$ is the cost function for the case with fixed location RNs. Thus, Proposition 3 is suitable for both the cases with fixed location and randomly distributed RNs.

Remark 3: Proposition 3 shows that the proposed iterative method may converge in the case of good GDOP and enough large N whereas it may diverge for the case of bad GDOP and small numbers of RNs. For a real channel environment, both bad and good GDOPs may coexist and the number of RNs is uncertainty. This means that the proposed iterative method cannot always converge. Thus, a hybrid location algorithm based on the proposed iterative method and closed-form solution is presented in Section.IV(C) to guarantee the convergence of the iterative method in bad channel situation. GDOP and convergence tests are proposed in the hybrid location algorithm to avoid the proposed method divergency.

Figure 3 and 4 show the cost function $J_r(\boldsymbol{\theta})$ for the case with good or bad GDOP. BN locates at the centroid of the RNs in Fig. 3 whereas BN is deployed outside of the RNs in Fig. 4. In both Figs. 3–4, $N = 4$, $\sigma = 10m$, and $\sigma_p = 30m$. It can be observed from Fig. 3 that there exists a unique global maximum for $J_r(\boldsymbol{\theta})$ in the case of good GDOP. For the better presentation, five points have been labeled in the Fig. 4. The coordinates of five points are (-79.1, -22.7), (-51.7, -22.7), (-19.9, -22.7), (3.5, -22.7), and (44.8, -22.7)

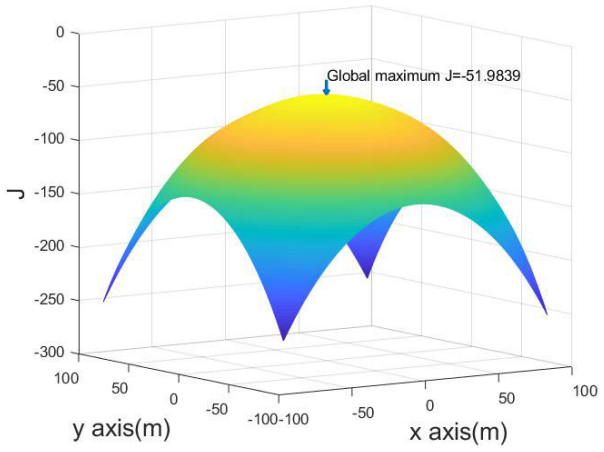

FIGURE 3. The cost function with good GDOP.

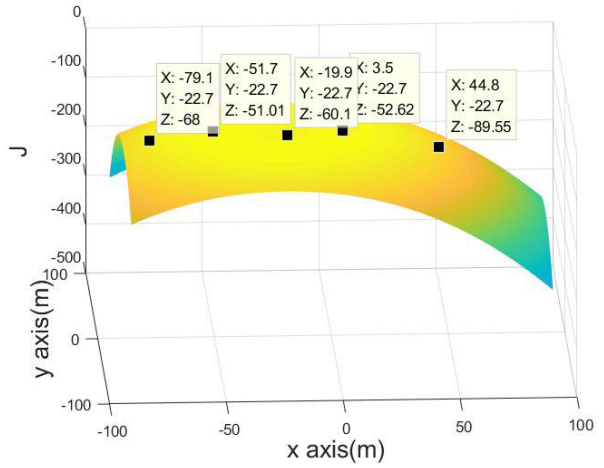

FIGURE 4. The cost function with bad GDOP.

while the corresponding cost function values are -68, -51.01, -60.1, -52.62, and -89.55. The y coordinates of five points are the same -22.7. Obviously, the third point (-19.9, -22.7) with J=-60.1 is a local minimum. Since the cost function of the iterative method is non-convex in the case of bad GDOP, the iterative method may converge to a local minimum in the bad channel situation.

For the case with good GDOP, iterative method can be used to obtain the higher positioning accuracy. A robust method should be developed to guarantee the convergence of iterative method in bad channel situation.

C. CLOSED FORM SOLUTION FOR THE CASE WITH RANDOMLY DISTRIBUTED RNS

It is well known that the iteration of Newton-Raphson may not converge. This will be particularly evident when $\mathbf{P}$ is a singular matrix in the case of bad GDOP. In this case it is seen from (45) that the correction term may fluctuate wildly from iteration to iteration.

As discussed in the Proposition 3, there may be local minimum in the case with bad GDOP and large TOA noise. Even if the iteration converges, the point found may not be the global maximum but possibly only a local minimum. Generally, if the initial point is close to the global maximum, the iteration will converge to it. Thus, a good initial guess is very important.

A closed-form solution based on MLE is developed here to provide an initial guess and is also used as the final estimate when the iteration does not converge.

Using simple mathematical manipulation and considering the TOA noise, the error vector derived from (42) is:

$$\mathbf{e} = \mathbf{Y} - \mathbf{GZ} \tag{51}$$

where

$$\mathbf{G} = \begin{bmatrix} 2x_1 & 2y_1 & -1 \\ \vdots & \vdots & \vdots \\ 2x_N & 2y_N & -1 \end{bmatrix}, \mathbf{Z} = \begin{bmatrix} x \\ y \\ k \end{bmatrix},$$

$$\mathbf{Y} = \begin{bmatrix} k_1 - \omega^2 \widehat{r}_1^2 \\ \vdots \\ k_N - \omega^2 \widehat{r}_N^2 \end{bmatrix},$$

$$\omega = \frac{\sigma_p^2}{\sigma_p^2 + \sigma^2}, k = x^2 + y^2, \text{ and } k_i = x_i^2 + y_i^2.$$

The first step MLE of $\mathbf{Z}$ can be obtained from (51):

$$\begin{aligned} \mathbf{Z} &= \arg\min \left\{ (\mathbf{Y} - \mathbf{GZ})^T \Psi^{-1} (\mathbf{Y} - \mathbf{GZ}) \right\} \\ &= \left(\mathbf{G}^T \Psi^{-1} \mathbf{G} \right)^{-1} \mathbf{G}^T \Psi^{-1} \mathbf{Y} \end{aligned} \tag{52}$$

where ψ is the covariance matrix of $\mathbf{e}$:

$$\psi = \text{cov}(\mathbf{e}) = E\left[\mathbf{e}\mathbf{e}^T\right] = \mathbf{BQB} \tag{53}$$

with $\mathbf{B} = 2\omega diag\{[r_1, \cdots, r_N]\}$, and $\mathbf{Q} = \sigma^2 \mathbf{I}$.

Since the covariance matrix ψ depends on the unknown r_i, further approximation is necessary in order to make the problem solvable. The approximate estimate of r_i can be obtained using LS estimator:

$$\mathbf{Z} = \left(\mathbf{G}^T \mathbf{G} \right)^{-1} \mathbf{G}^T \mathbf{Y} \tag{54}$$

$$r_i = \sqrt{(Z_1 - x_i)^2 + (Z_2 - y_i)^2} \tag{55}$$

cov($\mathbf{Z}$) is the covariance matrix of $\mathbf{Z}$ and can be obtained by using the perturbation approach. Δ is denoted as error perturbation. Expressing (52) by Taylor expansion, ignoring the square error term and retaining only the linear perturbation, $\Delta\mathbf{Z}$can be obtained:

$$\begin{aligned} \Delta\mathbf{Z} &= \left(\mathbf{G}^T \Psi^{-1} \mathbf{G} \right)^{-1} \mathbf{G}^T \Psi^{-1} \Delta\mathbf{Y} \\ &= \left(\mathbf{G}^T \Psi^{-1} \mathbf{G} \right)^{-1} \mathbf{G}^T \Psi^{-1} \mathbf{Bn} \end{aligned} \tag{56}$$

where $\mathbf{n} = \begin{bmatrix} n_1 \cdots n_N \end{bmatrix}^T$ is a vector of range measurement noise. Substituting (56) into cov($\mathbf{Z}$), the covariance matrix of

$\mathbf{Z}$ can be obtained:

$$\begin{aligned}\mathrm{cov}(\mathbf{Z}) &= E\left[\Delta\mathbf{Z}\Delta\mathbf{Z}^T\right] \\ &= \left(\mathbf{G}^T\Psi^{-1}\mathbf{G}\right)^{-1}\mathbf{G}^T\Psi^{-1}\mathbf{B}\mathbf{n}\mathbf{n}^T\mathbf{B}\Psi^{-1}\mathbf{G}\left(\mathbf{G}^T\Psi^{-1}\mathbf{G}\right)^{-1} \\ &= \left(\mathbf{G}^T\Psi^{-1}\mathbf{G}\right)^{-1} \end{aligned} \tag{57}$$

The estimation accuracy can be further improved using the relationship between x, y, and k. The first step solution of $\mathbf{Z}$ in (52) is based on the assumption of independent x, y, and k. However those parameters are correlated by $k = x^2 + y^2$. The results can be revised as follows using the relation of $k = x^2 + y^2$:

$$\mathbf{e}' = \mathbf{Y}' - \mathbf{G}'\mathbf{Z}' \tag{58}$$

where

$$\mathbf{Y}' = \begin{bmatrix} Z_1^2 \\ Z_2^2 \\ Z_3 \end{bmatrix}, \mathbf{G}' = \begin{bmatrix} 1 & 0 \\ 0 & 1 \\ 1 & 1 \end{bmatrix}, \mathbf{Z}' = \begin{bmatrix} x^2 \\ y^2 \end{bmatrix}.$$

Let the estimation errors of x, y, and k be μ_1, μ_2, and μ_3. Then the elements of $\mathbf{Z}$ become:

$$Z_1 = x + \mu_1, Z_2 = y + \mu_2, Z_3 = k + \mu_3 \tag{59}$$

Substituting (59) into (58) and ignoring the square error term, the entries of $\mathbf{e}'$ can be expressed as:

$$e_1' = 2x\mu_1, e_2' = 2y\mu_2, e_3' = \mu_3 \tag{60}$$

Subsequently, the covariance matrix of $\mathbf{e}'$ is:

$$\Psi' = E\left(\mathbf{e}'\mathbf{e}'^T\right) = \mathbf{B}'\mathrm{cov}(\mathbf{Z})\mathbf{B}' \tag{61}$$

where $\mathbf{B}' = diag\{[2x, 2y, 1]\}$. In fact, $\mathbf{B}'$ is unknown as $\mathbf{B}'$ contains the true BN position x and y. $\mathbf{B}'$ can be approximated as $\mathbf{B}' = diag\{[2Z_1, 2Z_2, 1]\}$.

The second step MLE solution is:

$$\mathbf{Z}' = \left(\mathbf{G}'^T\Psi'^{-1}\mathbf{G}'\right)^{-1}\mathbf{G}'^T\Psi'^{-1}\mathbf{Y}' \tag{62}$$

Similarly, the covariance matrix of $\mathbf{Z}'$ can be obtained by using the perturbation approach:

$$\mathrm{cov}(\mathbf{Z}') = \left(\mathbf{G}'^T\Psi'^{-1}\mathbf{G}'\right)^{-1} \tag{63}$$

The position estimation $\mathbf{Z}''$:

$$\mathbf{Z}'' = sign(\mathbf{Z})\sqrt{\mathbf{Z}'} \tag{64}$$

In summary, the steps of the proposed method can be listed as follow:

1) estimating ψ through substituting (55) into (53).
2) the first weight solution of BN can be obtained through substituting (53) into (52).
3) the final solution of BN can be obtained from (64).

From the definition of $\mathbf{Z}'$ in (58) and ignoring the square error term, $\mathbf{Z}'$ can be rewritten as:

$$Z_1' - x^2 = 2xe_x, Z_2' - y^2 = 2ye_y \tag{65}$$

where e_x and e_y are the estimation errors of x, y respectively. The covariance matrix of $\mathbf{Z}''$ can be obtained from (64):

$$\mathrm{cov}\left(\mathbf{Z}''\right) = \mathbf{B}''^{-1}\mathrm{cov}(\mathbf{Z}')\mathbf{B}''^{-1} \tag{66}$$

where $\mathbf{B}'' = diag\{[2x\ 2y]\}$.

From (57), (61), (63), and (66), the covariance matrix of $\mathbf{Z}''$ can be finally obtained:

$$\begin{aligned}\mathrm{cov}\left(\mathbf{Z}''\right) &= \left(\mathbf{B}''\mathrm{cov}(\mathbf{Z}')^{-1}\mathbf{B}''\right)^{-1} \\ &= \left(\mathbf{B}''\mathbf{G}'^T\Psi'^{-1}\mathbf{G}'\mathbf{B}''\right)^{-1} \\ &= \left(\mathbf{B}''\mathbf{G}'^T\mathbf{B}'^{-1}\mathrm{cov}(\mathbf{Z})^{-1}\mathbf{B}'^{-1}\mathbf{G}'\mathbf{B}''\right)^{-1} \end{aligned} \tag{67}$$

The covariance matrix $\mathrm{cov}\left(\mathbf{Z}''\right)$ will be used in the convergence test of the proposed hybrid method.

D. HYBRID LOCATION ALGORITHM COMBING THE ITERATIVE METHOD AND CLOSED-FORM SOLUTION

This subsection proposes a hybrid location algorithm based on the proposed iterative method and closed-form solution. The iterative method is used to provide the positioning results with high precision while its convergence is guaranteed by the closed-form solution.

(1) GDOP Test

As discussed in section.IV(B), the iterative method may diverge in the case of bad GDOP. The authors in [25] proved that the centroid of point RNs $\{(x_i, y_i)\}_{k=1}^N$ has the lowest GDOP. This means that the position near the centroid may have the better GDOP than a further point. Based on such observation, the following test is made to check whether the case has good or bad GDOP.

First, the centroid of point RNs can be calculated as:

$$x_{center} = \frac{1}{N}\sum_{i=1}^{N} x_i, y_{center} = \frac{1}{N}\sum_{i=1}^{N} y_i \tag{68}$$

The range between RN i and the centroid is:

$$r_{center\_i} = \sqrt{(x_{center} - x_i)^2 + (y_{center} - y_i)^2} \tag{69}$$

Second, the corresponding mean range is computing as:

$$\bar{r}_{center} = \frac{1}{N}\sum_{i=1}^{N} r_{center\_i} \tag{70}$$

The mean range is used to determine the coverage area of good GDOP. The initial estimate $\boldsymbol{\theta}_C = \left[x_c\ y_c\right]^T$ of BN can be obtained from the closed form solution (64). The range between the centroid and $\boldsymbol{\theta}_C$ is:

$$r_c = \sqrt{(x_c - x_{center})^2 + (y_c - y_{center})^2} \tag{71}$$

Finally, making the decision based on the following condition:

$$\begin{aligned} r_c &< \bar{r}_{center} \text{ for good GDOP} \\ r_c &\geq \bar{r}_{center} \text{ for bad GDOP} \end{aligned}$$

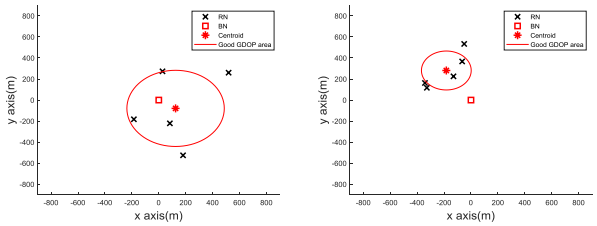

(a) Good GDOP (b) Bad GDOP

FIGURE 5. GDOP Test.

Fig. 5 shows the two cases with good and bad GDOPs. For good GDOP, the proposed iterative method is used to provide higher location accuracy. The estimate of BN's position obtained from the closed form solution is regarded as the final estimate in the case of bad GDOP. It can be seen from (68-71) that the GDOP test merely requires some simple algebraic manipulations. It not only makes sure the convergence of the iterative method in most cases but also reduces the computational burden since it avoids to apply the iterative method in the case of bad GDOP. Further assurance of the convergence is provided by convergence test in the next subsection.

(2) Convergence Test

Traditional Newton-Raphson method is based on the convergence condition $\boldsymbol{\theta}_{k+1} = \boldsymbol{\theta}_k$ and $g_1(\boldsymbol{\theta}_k) = g_2(\boldsymbol{\theta}_k) = 0$. It holds for the case that the cost function is a convex function. As shown in Fig. 4, the cost function is a nonconvex function in some situations. Further convergence test is required to avoid the proposed method divergency.

Since both the proposed iterative (45) and closed-form (64) estimators are based on MLE, the estimate errors of (45) and (64) can be approximated as Gaussian variables with zero mean. Assuming that $\boldsymbol{\theta}_I = \left[x_I \; y_I\right]^T$ and $\boldsymbol{\theta}_C = \left[x_C \; y_C\right]^T$ are the final estimates of (45) and (64) respectively, the estimate variance of closed-form solution (64) can be obtained from (67):

$$\begin{aligned}\sigma_C^2 &= Tr\left\{E\left[(\boldsymbol{\theta}_C - \boldsymbol{\theta})(\boldsymbol{\theta}_C - \boldsymbol{\theta})^T\right]\right\} \\ &= Tr\left\{\left(\mathbf{B}''\mathrm{cov}(\mathbf{Z}')^{-1}\mathbf{B}''\right)^{-1}\right\}\end{aligned} \tag{72}$$

where $\boldsymbol{\theta}$ is the true position of BN. For the proposed iterative method, it will asymptotically attain the CRLB when the iteration converges. Thus, the estimate variance of the iterative estimate (45) can be obtained from the proposed CRLB:

$$\sigma_I^2 = Tr\left\{E\left[(\boldsymbol{\theta}_I - \boldsymbol{\theta})(\boldsymbol{\theta}_I - \boldsymbol{\theta})^T\right]\right\} = \frac{4\sigma^2\sigma_p^2}{N\left(\sigma_p^2 + 2\sigma^2\right)} \tag{73}$$

Because both $\boldsymbol{\theta}_I$ and $\boldsymbol{\theta}_C$ are modeled as Gaussian variables with mean $\boldsymbol{\theta}$ and variances σ_I^2 and σ_C^2, $\boldsymbol{\theta}_I - \boldsymbol{\theta}_C$ is also a Gaussian random variance with mean and variance:

$$\begin{aligned}&E\left[\boldsymbol{\theta}_I - \boldsymbol{\theta}_C\right] = E\left[(\boldsymbol{\theta}_I - \boldsymbol{\theta}) - (\boldsymbol{\theta}_C - \boldsymbol{\theta})\right] \\ &\quad = E\left[\boldsymbol{\theta}_I - \boldsymbol{\theta}\right] - E\left[\boldsymbol{\theta}_C - \boldsymbol{\theta}\right] = 0 \\ &\sigma_{IC}^2 = Tr\left\{E\left[(\boldsymbol{\theta}_I - \boldsymbol{\theta}_C)(\boldsymbol{\theta}_I - \boldsymbol{\theta}_C)^T\right]\right\}\end{aligned} \tag{74}$$

$$\begin{aligned}&= Tr\left\{E\left[((\boldsymbol{\theta}_I - \boldsymbol{\theta}) - (\boldsymbol{\theta}_C - \boldsymbol{\theta}))((\boldsymbol{\theta}_I - \boldsymbol{\theta}) - (\boldsymbol{\theta}_C - \boldsymbol{\theta}))^T\right]\right\} \\ &= Tr\left\{E\left[(\boldsymbol{\theta}_I - \boldsymbol{\theta})(\boldsymbol{\theta}_I - \boldsymbol{\theta})^T\right] - E\left[(\boldsymbol{\theta}_I - \boldsymbol{\theta})(\boldsymbol{\theta}_C - \boldsymbol{\theta})^T\right]\right. \\ &\left. - E\left[(\boldsymbol{\theta}_C - \boldsymbol{\theta})(\boldsymbol{\theta}_I - \boldsymbol{\theta})^T\right] + E\left[(\boldsymbol{\theta}_C - \boldsymbol{\theta})(\boldsymbol{\theta}_C - \boldsymbol{\theta})^T\right]\right\} \\ &\approx \sigma_C^2 + \sigma_I^2\end{aligned} \tag{75}$$

Defining a random variable as:

$$\varsigma = \varsigma_x^2 + \varsigma_y^2 \tag{76}$$

where $\varsigma_x = \frac{x_C - x_I}{\sigma_{IC}/2}$ and $\varsigma_y = \frac{y_C - y_I}{\sigma_{IC}/2}$. Since ς_x and ς_y are subject to Gaussian distribution $N(0, 1)$, ς can be modeled as an exponential random variable with the PDF:

$$f(\varsigma) = \begin{cases} \frac{1}{2}\exp\left(-\frac{1}{2}\varsigma\right) & \varsigma > 0 \\ 0 & \varsigma < 0 \end{cases} \tag{77}$$

Based on exponential variable ς, constant false alarm detection (CFAR) is used here to detect the convergence of the proposed iterative method. P_{fa} is denoted as the probability of false alarm:

$$\begin{aligned}P_{fa} &= \Pr\{\varsigma > \gamma\} = \int_\gamma^{+\infty} \frac{1}{2}\exp\left(-\frac{1}{2}\varsigma\right) d\varsigma = -e^{-\frac{1}{2}\varsigma}\Big|_\gamma^{+\infty} \\ &= e^{-\frac{1}{2}\gamma}\end{aligned} \tag{78}$$

where γ is the threshold. The aim of CFAR is to constrain P_{fa} by choosing the threshold γ. From (78), γ can be calculated as:

$$\gamma = -2\ln P_{fa} \tag{79}$$

Generally, P_{fa} is set to be a small value to keep the lower false alarm.

Finally, the following judge condition can be used to determine whether the iterative method converges or diverges.

$$\begin{aligned}&\varsigma < \gamma \text{ for convergence case} \\ &\varsigma \geq \gamma \text{ for divergence case}\end{aligned}$$

For the case of convergence, $\boldsymbol{\theta}_I$ collected from the iterative method (45) is chose as the final estimate. Otherwise, the proposed method selects $\boldsymbol{\theta}_C$ as the location result.

When $P_{fa} \to 0, \gamma \to +\infty$ and the iterative method always works. Otherwise, the closed form solution is selected in the hybrid method for the case $P_{fa} \to 1$. Compared with the closed form solution, the iterative method has the higher positioning accuracy but it is easy to diverge. Obviously, the probability of false alarm P_{fa} provides a compromise between the positioning accuracy and divergence of the method. The effect of P_{fa} will be analyzed in the section V.

(3) Flowchart for the proposed hybrid algorithm

To illustrate, the main idea of the proposed hybrid location algorithm is as follows. The iterative method is easily to converge in the case of good GDOP. A GDOP test is firstly applied to judge whether starts the iterative method. This test is based on the observation that the centroid of point RNs has the best GDOP and is performed by comparing the range

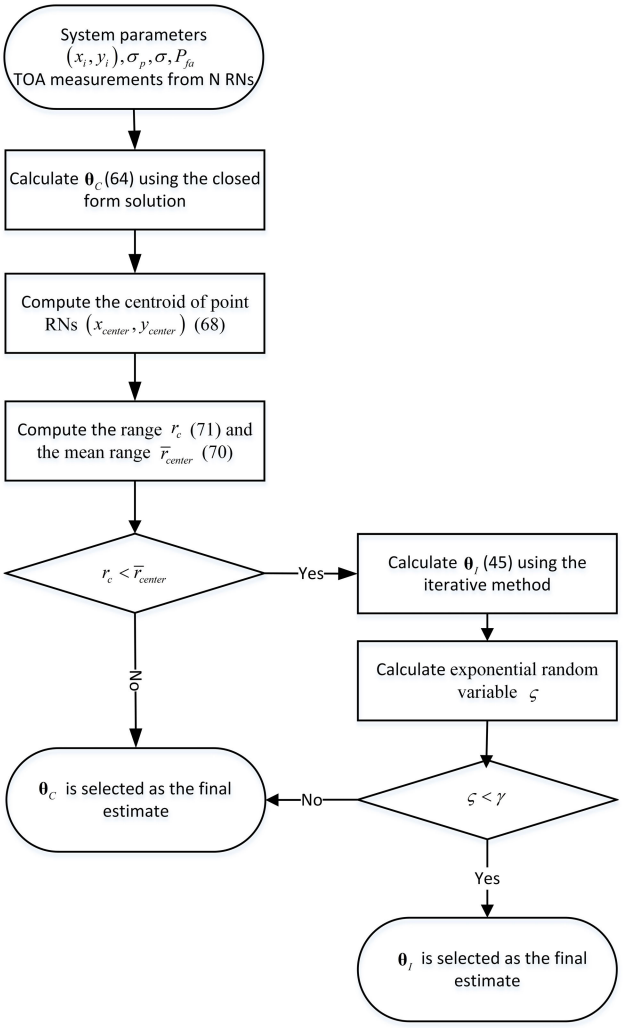

FIGURE 6. Flowchart for the proposed hybrid algorithm.

between the initial guess of BN and the centroid of point RNs with the mean range of RNs. If the iterative method is applied, convergence test is made to avoid the proposed method divergency. If the iterative method converges, the estimate difference between $\boldsymbol{\theta}_I - \boldsymbol{\theta}_C$ should have normalized residuals that obey the exponential distribution. The algorithm flow chart is in Fig. 6.

V. PERFORMANCE EVALUATION

In this section, we evaluate the performance of the TOA-based localization in 5G UDN with randomly distributed nodes and verify the accuracy of the analytical results obtained. The RMSEs are defined as $\sqrt{E\left[\left(x-\hat{x}\right)^2+\left(y-\hat{y}\right)^2\right]}$ in the units of m. The statistical results are obtained from the average of 10000 independent runs.

A. CRLB ANALYSIS

Three CRLBs are compared in this subsection, which include the proposed CRLB (27) for randomly distributed nodes and the two traditional CRLBs (15) and (16) for fixed

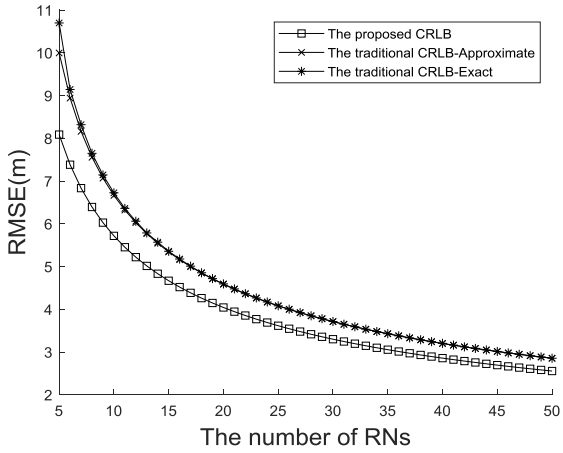

FIGURE 7. CRLB comparisons versus different N.

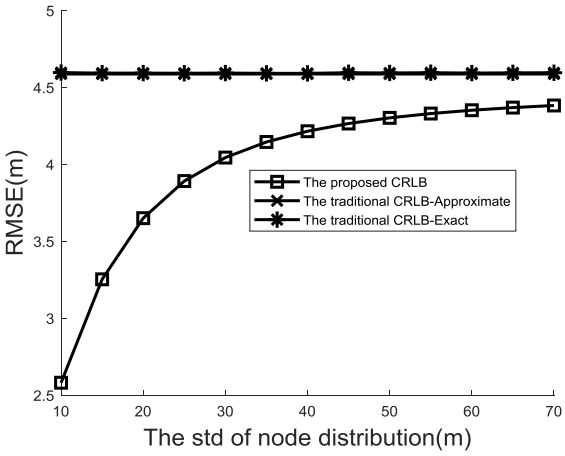

FIGURE 8. CRLB comparisons versus different σ_p.

location RNs. The difference between (15) and (16) is that the latter approximates the former in the case with enough large N.

Fig. 7 is performed to study the impact of the number of RNs on the positioning accuracy. In this figure, N varies from 5 to 50, $\sigma = 10m$ and $\sigma_p = 30m$. For the traditional CRLBs (15) and (16), (16) asymptotically attains (15) when $N > 12$. Thus, (15) can be replaced with (16) for large N. As the number of RNs increases, the CRLBs decrease. Even with medium range measurement error $\sigma = 10m$, both the proposed and traditional CRLBs can reach meter level positioning accuracy in the case of large N. This conclusion is very useful for UDNs. Take 5G as example, it is normal for a BN with dozens of connected devices. In this case, an acceptable positioning accuracy can be achieved even in bad channel environment. For RMSE 4m, N are equal to 20 and 26 for the proposed CRLB and traditional CRLB. This means that the prior information $\sigma_p = 30m$ on the spatial node distribution can reduce 6 RNs.

Fig. 8 is plotted to compare the CRLBs with different stds σ_p of RNs distribution when $\sigma = 10m$ and $N = 20$. With the fixed N and σ, the traditional CRLB is a constant value whereas the positioning accuracy of the proposed

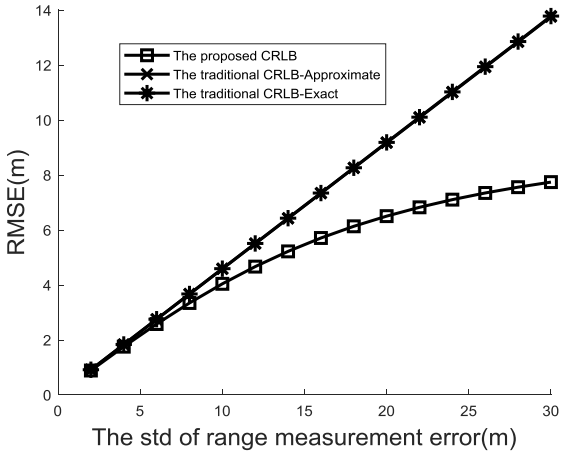

FIGURE 9. CRLB comparisons versus different σ.

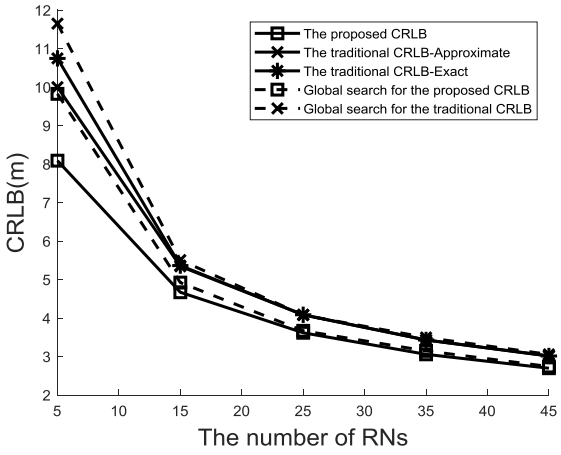

FIGURE 10. Comparisons between the global search methods and CRLBs.

CRLB becomes better as σ_p decreases. This means that the traditional CRLB only relies on the range measurement error σ whereas both σ and σ_p will affect the proposed CRLB. It also can be observed that the main distributed area of RNs becomes small with the decreasing σ_p and the small distributed area of RNs will help to improve the system performance for the case of randomly distributed RNs. This means that the proposed methods are very suitable for 5G UDN with short communication range.

Fig. 9 is recorded to compare the CRLBs with different stds σ of range measurement error when $\sigma_p = 30m$ and $N = 20$. The std σ of range measurement error varies from 2m to 30m. Although both CRLBs increase as σ increases as shown in Fig. 9, the rising tendency of the proposed CRLB is slower than those of the traditional CRLBs. This is because the proposed CRLB not only depends on σ but also is constrained by σ_p. In the case of high precision range estimate $\sigma \leq 6m$, the two CRLBs almost have the same positioning accuracy. However, the proposed CRLB has the larger advantage when $\sigma \geq 10m$. It should be noted that high precision range estimate relies on time synchronization. For $\sigma = 6m$, the time synchronization error should be smaller than 20ns. Even for 5G system, it is a hard work. Thus, the proposed method using the distributed area σ_p to improve the location accuracy is a preferred solution.

All of Figs. 7–9 show that the proposed CRLB is smaller than the traditional CRLBs (15) and (16) which matches the analysis result obtained from Proposition 1.

The effectiveness of the proposed CRLB is evaluated in Fig. 10. It is well known that the MLE is asymptotically efficient and optimal with sufficiently large measurements. Thus, global search methods based on ML cost function are compared with the three CRLBs in this simulation.

For the traditional CRLBs, the MLE objective function of global search method is:

$$J_f(\boldsymbol{\theta}) = \max_{x,y} \left(-\left(N \ln\left(\sqrt{2\pi}\sigma\right) + \sum_{i=1}^{N} \frac{\left(\widehat{r}_i - r_i\right)^2}{2\sigma^2} \right) \right) \tag{80}$$

For the proposed CRLB, the MLE objective function of global search method is:

$$J_r(\boldsymbol{\theta}) = \max_{x,y} \left(-\left(N \ln\left(\sqrt{2\pi}\sigma\right) + \sum_{i=1}^{N} \frac{\left(\widehat{r}_i - r_i\right)^2}{2\sigma^2} \right) - \left(N \ln\left(2\pi\sigma_p^2\right) + \sum_{i=1}^{N} \frac{r_i^2}{2\sigma_p^2} \right) \right) \tag{81}$$

The search gap for both (80) and (81) is 0.1m. Fig. 10 shows the performance comparisons between the global search methods and three CRLBs. In Fig. 10, N varies from 5 to 45, $\sigma = 10m$ and $\sigma_p = 30m$. It shows that global search methods can reach the corresponding CRLBs after $N \geq 15$. This means the MLE methods can asymptotically attain the traditional and proposed CRLBs as N increases. This conclusion matches the asymptotical property of MLE method [55] and verifies the effectiveness of the proposed and traditional CRLBs.

B. PERFORMANCE OF THE PROPOSED METHODS

The first simulation set of this subsection is to check the convergence of the iterative method. Proposition 3 has verified that both the cost functions of the proposed and traditional iterative methods are asymptotical convex function in the case of enough large N. The proposed iterative method (45) and the traditional iterative method in [10] are compared in Fig. 11. The former is proposed for the case of randomly distributed RNs whereas the latter is derived for that of the fixed location RNs. In Fig. 11, N varies from 5 to 13, $\sigma = 10m$ and $\sigma_p = 30m$. It is shown that both diverge with the small N ($N \leq 8$). As the N increases, both algorithms become converging which matches the analysis results obtained from Proposition 3. Fig. 11 also shows that the proposed iterative method is more robust than the traditional method. Since both algorithms diverge with small N, the hybrid method is proposed in this paper to guarantee the convergence of the iterative algorithm.

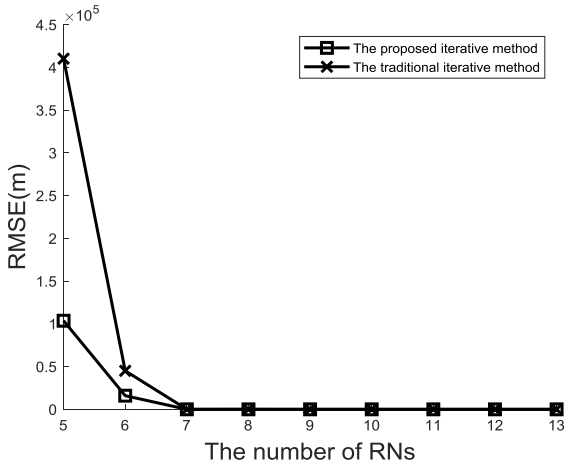

FIGURE 11. Convergence analysis of the iterative methods.

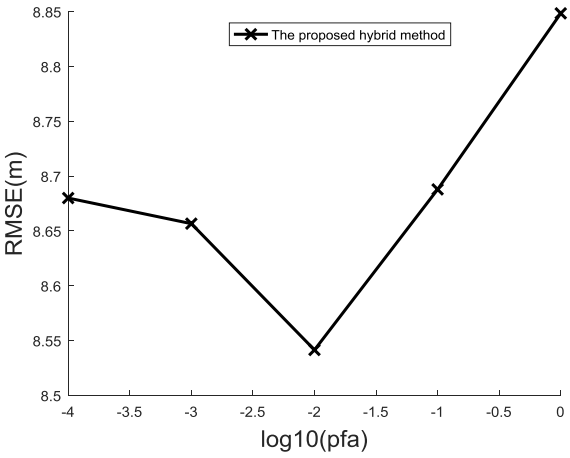

FIGURE 12. The effect of the probability of false alarm P_{fa}.

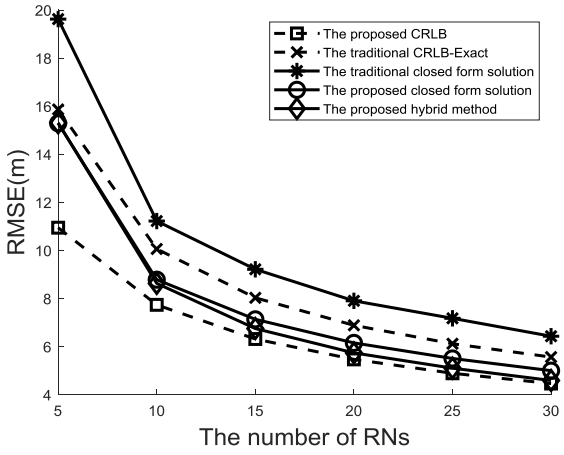

FIGURE 13. Performance comparisons versus different numbers of RNs.

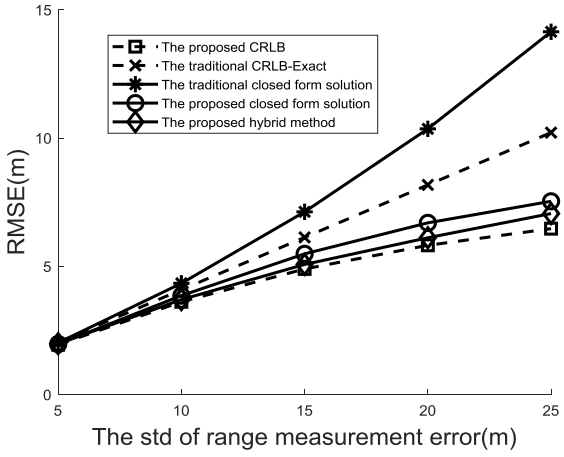

FIGURE 14. Performance comparisons versus different stds of range measurement error.

The effect of the probability of false alarm P_{fa} is analyzed in Fig. 12. P_{fa} varies from 10^{-4} to 1, $\sigma = 15m$, $\sigma_p = 30m$ and $N = 10$. It can be seen from the figure that the proposed hybrid method obtains the highest positioning accuracy when $P_{fa} = 0.01$. Thus, P_{fa} is set to be 0.01 in our algorithm.

Performance comparisons of the proposed methods are recorded in the following figures. Three location methods including the proposed closed form estimator, the proposed hybrid method, and the traditional location method with closed form solution for fixed location RNs [18] are compared in the simulation. The proposed and traditional CRLBs are also included in the figures.

Fig. 13 shows the performance comparisons of various location methods and CRLBs in the case with different numbers of RNs. In this figure, the number of RNs varies from 5 to 30, $\sigma = 15m$ and $\sigma_p = 30m$. It can be observed that the proposed hybrid algorithm provides the best performance in all cases and can asymptotically attain the proposed CRLB. This means that the proposed hybrid algorithm can effectively suppress the divergence of the iterative method and obtain the good positioning accuracy. Moreover, the proposed closed form solution also outperforms than the traditional CRLB and closed form estimator.

Fig. 14 is plotted to evaluate the performance in the case with different stds of range measurement error. The std of range measurement error σ varies from 5m to 25m, $N = 25$ and $\sigma_p = 30m$. Although all of the methods and CRLBs increase as σ increases, the rising tendency of the proposed algorithms and CRLB is slower than those of the traditional CRLB and method. This implies that the proposed method can effectively utilize the prior information on RN distribution to get a robust and higher precision location estimate especially in bad channel situation with low range estimated accuracy.

Fig. 15 is simulated to compare the performance of methods in the case with different stds σ_p of RN distribution. In Fig. 15, σ_p varies from 10m to 55m, $N = 30$ and $\sigma = 10m$. The figure shows that the proposed hybrid method can reach the proposed CRLB with various σ_p whereas the traditional closed form solution has a large location error for the case with small σ_p and asymptotically attains the traditional CRLB as σ_p increases. This is because the GDOP of the tradition method becomes better as σ_p/σ increases. Compared with

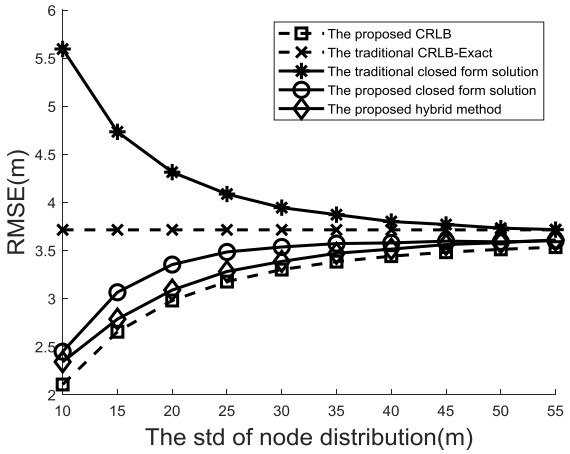

FIGURE 15. Performance comparisons versus different stds of node distribution.

the traditional method, the proposed methods work well in different σ_p. The simulation result proves that the proposed methods is more robust in the bad channel environment.

All of Figs. 13–15 show that the proposed methods including hybrid estimator and closed form solution perform better than the traditional CRLB and closed form method which verifies the effectiveness of the proposed methods.

VI. CONCLUSION

Although node randomness has been considered in the localization of 5G UDN, it is only used in current research to evaluate the average performance such as averaged area of location region, theoretical variance, and the average CRLB. This paper proposes a CRLB and three location algorithms considering both the range measurements and the distribution of RNs, which answer the two unsolvable questions of localization in 5G UDN: what is the best achievable positioning accuracy of 5G UDN with randomly distributed RNs? and How to obtain the corresponding optimum positioning estimator using the prior information on RNs distribution? Some characteristics of the CRLB for 5G UDN localization are derived in the paper. Detail comparison between our study and the previous research of CRLB for 5G UDN is also given. Because of the effective utilization of the prior information on RNs distribution, the proposed algorithms provide the better performance than the traditional methods merely using the range measurements. An analysis that incorporates the distribution of RNs, prior user location knowledge, and RN location error will be left for a future study.

ACKNOWLEDGMENT

The authors would like to thank the anonymous referees for their suggestions and comments.

REFERENCES

[1] B. P. Zhou, A. Liu, and V. Lau, "Successive localization and beamforming in 5G mmWave MIMO communication systems," *IEEE Trans. Signal Process.*, vol. 67, no. 6, pp. 1620–1635, Mar. 2019.

[2] S. Safavi, U. A. Khan, S. Kar, and J. M. F. Moura, "Distributed localization: A linear theory," *Proc. IEEE*, vol. 106, no. 7, pp. 1204–1223, Jul. 2018.

[3] J. H. Reed, K. J. Krizman, B. D. Woerner, and T. S. Rappaport, "An overview of the challenges and progress in meeting the E-911 requirement for location service," *IEEE Commun. Mag.*, vol. 36, no. 4, pp. 30–37, Apr. 1998.

[4] *Wireless E911 Location Accuracy Requirements*, document FCC 15-9, Feb. 2015.

[5] H. Kim, S. H. Lee, and S. Kim, "Cooperative localization with distributed ADMM over 5G-based VANETs," in *Proc. IEEE Wireless Commun. Netw. Conf. (WCNC)*, Barcelona, Spain, Apr. 2018, pp. 612–616.

[6] W. J. Yuan, N. Wu, Q. H. Guo, X. J. Huang, Y. H. Li, and L. Hanzo, "TOA-based passive localization constructed over factor graphs: A unified framework," *IEEE Trans. Commun.*, vol. 67, no. 10, pp. 6952–6965, Oct. 2019.

[7] Y. Xiong, N. Wu, Y. Shen, and M. Z. Win, "Cooperative network synchronization: Asymptotic analysis," *IEEE Trans. Signal Process.*, vol. 66, no. 3, pp. 757–772, Feb. 2018.

[8] D. J. Torrieri, "Statistical theory of passive location systems," *IEEE Trans. Aerosp. Electron. Syst.*, vol. AES-20, no. 2, pp. 183–197, Mar. 1984.

[9] M. A. Spirito, "On the accuracy of cellular mobile station location estimation," *IEEE Trans. Veh. Technol.*, vol. 50, no. 3, pp. 674–685, May 2001.

[10] J. Caffery and G. L. Stuber, "Subscriber location in CDMA cellular networks," *IEEE Trans. Veh. Technol.*, vol. 47, no. 2, pp. 406–416, May 1998.

[11] M. Hellebrandt, R. Mathar, and M. Scheibenbogen, "Estimating position and velocity of mobiles in a cellular radio network," *IEEE Trans. Veh. Technol.*, vol. 46, no. 1, pp. 65–71, Feb. 1997.

[12] J. J. Caffery, "A new approach to the geometry of TOA location," in *Proc. IEEE Veh. Technol. Conf.*, Boston, MA, USA, Sep. 2000, pp. 1943–1949.

[13] J. S. Abel, "A divide and conquer approach to least-squares estimation," *IEEE Trans. Aerosp. Electron. Syst.*, vol. 26, no. 2, pp. 423–427, Mar. 1990.

[14] B. Friedlander, "A passive localization algorithm and its accuracy analysis," *IEEE J. Ocean. Eng.*, vol. OE-12, no. 1, pp. 234–245, Jan. 1987.

[15] Y. T. Chan and K. C. Ho, "A simple and efficient estimator for hyperbolic location," *IEEE Trans. Signal Process.*, vol. 42, no. 8, pp. 1905–1915, Aug. 1994.

[16] J. Y. Huang, P. Liu, W. Lin, and G. Gui, "RSS-based method for sensor localization with unknown transmit power and uncertainty in path loss exponent," *Sensors*, vol. 16, no. 9, pp. 1–17, Sep. 2016.

[17] J. Y. Huang, "Calculation of mobile location based on TOA/SS measurements," *KSII Trans. Internet Inf. Syst.*, vol. 6, no. 12, pp. 3166–3181, 2012.

[18] F. K. W. Chan and H. So, "Accurate distributed range-based positioning algorithm for wireless sensor networks," *IEEE Trans. Signal Process.*, vol. 57, no. 10, pp. 4100–4105, Oct. 2009.

[19] F. K. W. Chan, H. C. So, J. Zheng, and K. W. K. Lui, "Best linear unbiased estimator approach for time-of-arrival based localisation," *IET Signal Process.*, vol. 2, no. 2, pp. 156–162, Jun. 2008.

[20] K. W. Cheung and H. C. So, "A multidimensional scaling framework for mobile location using time-of-arrival measurements," *IEEE Trans. Signal Process.*, vol. 53, no. 2, pp. 460–470, Feb. 2005.

[21] S. Kumar, R. Kumar, and K. Rajawat, "Cooperative localization of mobile networks via velocity-assisted multidimensional scaling," *IEEE Trans. Signal Process.*, vol. 64, no. 7, pp. 1744–1758, Apr. 2016.

[22] H. C. So and F. K. W. Chan, "A generalized subspace approach for mobile positioning with time-of-arrival measurements," *IEEE Trans. Signal Process.*, vol. 55, no. 10, pp. 5103–5107, Oct. 2007.

[23] H. W. Wei, Q. Wan, Z. X. Chen, and S. F. Ye, "A novel weighted multidimensional scaling analysis for time-of-arrival-based mobile location," *IEEE Trans. Signal Process.*, vol. 56, no. 7, pp. 3018–3022, Jul. 2008.

[24] W. Cui, C. D. Wu, W. Meng, B. Li, Y. Z. Zhang, and L. H. Xie, "Dynamic multidimensional scaling algorithm for 3-D mobile localization," *IEEE Trans. Instrum. Meas.*, vol. 65, no. 12, pp. 2853–2865, Oct. 2016.

[25] N. Levanon, "Lowest GDOP in 2-D scenarios," *IEE Proc.—Radar, Sonar Navigat.*, vol. 147, no. 3, pp. 149–155, Jun. 2000.

[26] D. H. Shin and T. K. Sung, "Comparisons of error characteristics between TOA and TDOA positioning," *IEEE Trans. Aerosp. Electron. Syst.*, vol. 38, no. 1, pp. 307–310, Jan. 2002.

[27] N. Patwari, A. O. Hero, III, M. Perkins, N. S. Correal, and R. J. O'Dea, "Relative location estimation in wireless sensor networks," *IEEE Trans. Signal Process.*, vol. 51, no. 8, pp. 2137–2148, Aug. 2003.

[28] J. Chaffee and J. Abel, "GDOP and the Cramér-Rao bound," in *Proc. IEEE Position Location Navigat. Symp.*, Apr. 1994, pp. 663–668.

[29] I. Guvenc, C.-C. Chong, F. Watanabe, and H. Inamura, "NLOS identification and weighted least-squares localization for UWB systems using multipath channel statistics," *EURASIP J. Adv. Signal Process.*, vol. 2008, Jul. 2008, Art. no. 271984.

[30] S. Maransò, W. M. Gifford, H. Wymeersch, and M. Z. Win, "NLOS identification and mitigation for localization based on UWB experimental data," *IEEE J. Sel. Areas Commun.*, vol. 28, no. 7, pp. 1026–1035, Sep. 2010.
[31] P.-C. Chen, "A non-line-of-sight error mitigation algorithm in location estimation," in *Proc. IEEE WCNC*, New Orleans, LA, USA, Sep. 1999, pp. 316–320.
[32] W. Kim, J. G. Lee, and G. I. Jee, "The interior-point method for an optimal treatment of bias in trilateration location," *IEEE Trans. Veh. Technol.*, vol. 55, no. 4, pp. 1291–1301, Jul. 2006.
[33] W. Cui, B. Li, L. Zhang, and W. Meng, "Robust mobile location estimation in NLOS environment using GMM, IMM, and EKF," *IEEE Syst. J.*, vol. 13, no. 3, pp. 3490–3500, Sep. 2019.
[34] Z. Abu-Shaban, X. Zhou, and T. D. Abhayapala, "A novel TOA-based mobile localization technique under mixed LOS/NLOS conditions for cellular networks," *IEEE Trans. Veh. Technol.*, vol. 65, no. 11, pp. 8841–8853, Nov. 2016.
[35] K. T. Feng, C. L. Chen, and C. H. Chen, "GALE: An enhanced geometry-assisted location estimation algorithm for NLOS environments," *IEEE Trans. Mobile Comput.*, vol. 7, no. 2, pp. 199–213, Feb. 2008.
[36] F. Lemic, V. Handziski, M. Aernouts, T. Janssen, R. Berkvens, A. Wolisz, and J. Famaey, "Regression-based estimation of individual errors in fingerprinting localization," *IEEE Access*, vol. 7, pp. 33652–33664, 2019.
[37] V. Moghtadaiee, S. A. Ghorashi, and M. Ghavami, "New reconstructed database for cost reduction in indoor fingerprinting localization," *IEEE Access*, vol. 7, pp. 104462–104477, 2019.
[38] A. R. L. Paiva, W. C. Freitas, I. M. Guerreiro, and H. J. B. Nascimento, "Indoor localization algorithm based on fingerprint using a single fifth generation Wi-Fi access point," *IEEE Latin Amer. Trans.*, vol. 16, no. 7, pp. 2020–2026, Jul. 2018.
[39] Y. Y. Jin, W.-S. Soh, and W.-C. Wong, "Indoor localization with channel impulse response based fingerprint and nonparametric regression," *IEEE Trans. Wireless Commun.*, vol. 9, no. 3, pp. 1120–1127, Mar. 2010.
[40] H. Miao, K. Yu, and M. Juntti, "Positioning for NLOS propagation: Algorithm derivations and Cramér-Rao bounds," *IEEE Trans. Veh. Technol.*, vol. 56, no. 5, pp. 2568–2580, Sep. 2007.
[41] Y. Qi, H. Kobayashi, and H. Suda, "Analysis of wireless geolocation in a non-line-of-sight environment," *IEEE Trans. Wireless Commun.*, vol. 5, no. 3, pp. 672–681, Mar. 2006.
[42] A. Behnad, X. Wang, L. Hanzo, and T. J. Willink, "Connectivity-based centroid localization using distributed dense reference nodes," *IEEE Trans. Veh. Technol.*, vol. 67, no. 7, pp. 6685–6689, Jul. 2018.
[43] J. D. Roth, M. Tummala, and J. C. McEachen, "Fundamental implications for location accuracy in ultra-dense 5G cellular networks," *IEEE Trans. Veh. Technol.*, vol. 68, no. 2, pp. 1784–1795, Feb. 2019.
[44] E. Y. Menta, N. Malm, R. Jäntti, K. Ruttik, M. Costa, and K. Leppänen, "On the performance of AoA–based localization in 5G ultra-dense networks," *IEEE Access*, vol. 7, pp. 33870–33880, 2019.
[45] H. Elsawy, W. Dai, M. Alouini, and M. Z. Win, "Base station ordering for emergency call localization in ultra-dense cellular networks," *IEEE Access*, vol. 6, pp. 301–315, 2018.
[46] T. Jia and R. M. Buehrer, "A new Cramér-Rao lower bound for TOA-based localization," in *Proc. IEEE Military Commun. Conf.*, San Diego, CA, USA, Nov. 2008, pp. 1–5.
[47] E. G. Larsson, "Cramér-Rao bound analysis of distributed positioning in sensor networks," *IEEE Signal Process. Lett.*, vol. 11, no. 3, pp. 334–337, Mar. 2004.
[48] C. Chang and A. Sahai, "Cramér-Rao-type bounds for localization," *EURASIP J. Appl. Signal Process.*, vol. 58, no. 7, pp. 1–13, Jul. 2006.
[49] K. W. K. Lui, W.-K. Ma, H. C. So, and F. K. W. Chan, "Semi-definite programming algorithms for sensor network node localization with uncertainties in anchor positions and/or propagation speed," *IEEE Trans. Signal Process.*, vol. 57, no. 2, pp. 752–763, Feb. 2009.
[50] K. Yu and Y. J. Guo, "Anchor global position accuracy enhancement based on data fusion," *IEEE Trans. Veh. Technol.*, vol. 58, no. 3, pp. 1616–1623, Mar. 2008.
[51] J. Y. Huang, P. Wang, and Q. Wan, "CRLBs for WSNs localization in NLOS environment," *EURASIP J. Wireless Commun. Netw.*, vol. 2011, p. 16, Dec. 2011, doi: 10.1186/1687-1499-2011-16.
[52] J. Y. Huang, Q. Wan, and P. Wang, "Minimum mean square error estimator for mobile location using time-difference-of-arrival measurements," *IET Radar, Sonar Navigat.*, vol. 5, no. 2, pp. 137–143, Feb. 2011.
[53] M. F. A. Ahmed and S. A. Vorobyov, "Collaborative beamforming for wireless sensor networks with Gaussian distributed sensor nodes," *IEEE Trans. Wireless Commun.*, vol. 8, no. 2, pp. 638–643, Feb. 2009.
[54] M. Michalopoulou and P. Mähönen, "The critical range in clustered ad hoc networks: An analysis for Gaussian distributed nodes," *IEEE Commun. Lett.*, vol. 19, no. 5, pp. 811–814, May 2015.
[55] S. M. Kay, *Fundamentals of Statistical Signal Processing: Estimation Theory*. Englewood Cliffs, NJ, USA: Prentice-Hall, 1993.
[56] R. A. Horn and C. R. Johnson, *Matrix Analysis*. Cambridge, U.K.: Cambridge Univ. Press, 1999.
[57] M. Grant and S. Boyd. (May 2010). CVX: MATLAB software for disciplined convex programming, version 1.21. CVX Research, Austin, TX, USA. [Online]. Available: http://cvxr.com/cvx

JIYAN HUANG was born in Jiangxi, China, in September 1981. He received the B.Eng. degree (Hons.) and the M.Eng. and Ph.D. degrees from the University of Electronic Science and Technology of China (UESTC), Chengdu, China, in 2003, 2005, and 2008, respectively. From 2008 to 2011, he was a Research Fellow with Nanyang Technological University, Singapore. He is currently an Associate Professor with the School of Information and Communication Engineering, UESTC. His research interests include statistical signal processing, detection and estimation, mobile localization and tracking, and radar signal processing.

JING LIANG received the B.S. and M.S. degrees in electrical engineering from the Beijing University of Posts and Telecommunications, Beijing, China, in 2003 and 2006, respectively, and the Ph.D. degree in electrical engineering from The University of Texas at Arlington, Arlington, TX, USA, in 2009. She is currently an Associate Professor with the Department of Electronic Engineering, University of Electronic Science and Technology of China, Chengdu, China. Her current research interests include radar sensor networks, collaborative and distributed signal processing, wireless communications, compressive sensing, wireless networks, and fuzzy logic systems.

SHAN LUO received the bachelor's degree in electrical information engineering and the master's degree in signal and information processing from the University of Electronic Science and Technology of China (UESTC), Chengdu, Sichuan, China, in 2007 and 2010, respectively, and the Ph.D. degree in information engineering from Nanyang Technological University, in 2014. She is currently an Associate Professor with the School of Aeronautics and Astronautics, UESTC. Her research interests include wireless communications, signal processing, and time-frequency analysis.